SPRFMO
South Pacific Regional Fisheries Management Organisation

11th MEETING OF THE SCIENTIFIC COMMITTEE

11 to 16 September 2023, Panama City, Panama

SC11 – Obs03 _rev1

Regional Assessment of the Jumbo Squid in the South-Eastern Pacific with Peruvian, Chilean and Asian fleets data and Impacts of El Niño Environmental Cycle: 1969 to 2020

CALAMASUR

Regional Assessment of the Jumbo Squid in the South-Eastern Pacific with Peruvian, Chilean and Asian fleets data and impacts of El Niño Environmental Cycle: 1969 to 2021

Authors

Rubén H. Roa-Ureta and Rodrigo Wiff
CALAMASUR Scientific Advisors

September 16, 2023

Acknowledgements. The authors would like to acknowledge the SPRFMO Secretariat and Delegations. Special thanks are given to the Chilean and Chinese authorities for providing their data. Acknowledgements are also given to the Peruvian government for providing their data via the state transparency platform. Thanks to the authorities of Taiwan and South Korean governments for providing their data via the SPRFMO Secretariat. The authors would like to acknowledge the initiative of CALAMASUR and the funding support provided by the Sustainable Fisheries Partnership in their efforts oriented to science-based fisheries management. This independent evaluation would not be possible without this multi stakeholder collaboration.

Contents

Executive Summary

The jumbo squid fishery is the largest invertebrate fishery in the world and one of the largest including finfish fisheries. In the South East Pacific Ocean (SEP) it is fished in four regions: (i) Ecuadorian, (ii) Peruvian and (iii) Chilean exclusive economic zones (EEZ), and (iv) international waters in the high seas west of those EEZs. In the high seas, the main operators currently are Chinese ships, while Chinese Taipei ships operated until 2020 and South Korean ships until 2019. During the last two years, the jumbo squid Working Group of the South Pacific Regional Fisheries Management Organization (SPRFMO) has led efforts to build standardized databases for regional stock assessment with contributions from all SPRFMO Commission Members fishing the jumbo squid in the SEP. We present here a stock assessment methodology and its application to a database built by CALAMASUR through these collaborative efforts. This methodology consists of two stages. At stage 1, a database of catches, fishing effort and mean weight of squids in the catch was built to apply multi-annual and multi-fleet depletion models at monthly time steps, covering the period of January 2012 to December 2021 for Chilean, Peruvian and Asian fleets. This part of the methodology followed the advice of a review article recently published by experienced cephalopod fisheries scientists. At Stage 2, a generalized surplus production utilized (i) the total annual landings across the SEP from 1969 to 2021 and (ii) predicted monthly biomass and its standard error from the depletion model (stage 1) using a hierarchical statistical inference framework to fit parameters of the population dynamics and biomass productivity of the stock. At stage 2 the assessment took into account the El Niño environmental cycle in the SEP with models having time-varying parameters. NOAA's ENSO index was used to define six environmental phases during our study period. Time-varying parameters on each phase led to eight alternative hypotheses describing increasingly complex changes in the carrying capacity of the environment, the symmetry of the production function, and the intrinsic rate of population growth.

Results of the multi-annual, multi-fleet depletion models at stage 1, show adequate fits with satisfactory residuals and quantile diagnostics. Natural mortality was estimated at 1.9332 per year with good statistical precision, and escapement biomass (January 2022) at 2.5 million tonnes. Recruitment has been decreasing for the Peruvian fleets, increased substantially in 2016 for the Asian fleets, and despite a high value in 2019, has fluctuated widely for the Chilean fleets. Biomass has wide intra-annual fluctuations, with maxima one order of magnitude higher than minima, and it has a decreasing trend in the last 2 years (2020 and 2021). Fishing mortality has been increasing but it stil remains under natural mortality. Current exploitation rates are close to 40%.

Results of the time-varying parameters surplus production model at stage 2 support the hypothesis that only the intrinsic rate of population growth varies between environmental phases although hypotheses that include changes in the carrying capacity of the environment and the symmetry of the production function may become supported as the database to fit the depletion model grows to include the data from fishing in 2022 and onward. Parameters of the best supported hypothesis were estimated with good precision though sustainable harvest rates based on the total latent productivity are still imprecise. The stock has entered a regime of wide fluctuations making the MSY and B_{MSY} inadequate reference points.

Overall, results of both the depletion model as well as the surplus production model indicate that the stock is being harvested in a sustainable manner, not over-fished and not undergoing over-fishing, but close to maximum capacity. Wide intra-annual fluctuations coild be a matter of concern for managers of the jumbo squid stock in the SEP.

Results from this stock assessment methodology can be improved by extending the times series of catch, effort and mean weights up to 2022 from Peruvians fleets and by extending the depletion model to include different natural mortality rates by the squids captured by the different fleets, to partially accommodate the known biological composition of the stock in three phenotypes, thus adding biological realism.

1 Introduction

The jumbo squid (*Dosidicus gigas*) fishery extends over the whole Eastern Pacific Ocean yielding the largest volume of annual landings of any invertebrate fishery worldwide, over a million tonnes in recent years [1]. This species is widely distributed in the Eastern Pacific, ranging approximately from 45^o N to 45^o S along the continental slope and extending to oceanic waters on the south east pacific up to 140^oW [2], inhabiting from the surface down to depths of 1200 m [3]. The highest abundance of flying jumbo squid are found off Peruvian and Chilean coasts. According to FAO records [4], in the South Eastern Pacific Ocean (SEP) the fishery started to develop and grow in the early 90s, with the activities of Japanese and Korean fleets in international waters off the jurisdiction of Ecuador, Peru and Chile, and Peruvian fleets in Peru's Exclusive Economic Zone (EEZ). Starting in the 2000s, Chilean and Chinese fleets joined the exploitation in Chilean EEZ and international waters, respectively, and in 2014 Ecuadorian fleets became active in the fishery.

During the last decade, biological attributes regarding age and growth [5], reproduction [6], mortality [7], feeding [8], predators [9], and the connection between volume of catches and environmental conditions [10, 1] have been reported. In recent years, discussions regarding method to assess jumbo squid and efforts toward sharing and standardizing databases have been made among SPRFMO Commission Members fishing jumbo squid in the SEP [11, 12], including a first attempt for a conceptualisation [13] and implementation [14] of region-wide stock assessment. In spite of these efforts, there is still need of an integrated system of observation, assessment and management to secure the continued viability of the fishery [15]. Currently, there is much interest in generating scientific knowledge leading to an assessment of the abundance and productive capacity of the stock in the SEP region as a whole. This knowledge would be useful to take coordinated management actions aimed at the sustainable exploitation of the stock by the various fleets and SPRFMO Commission Members involved.

Life history and stock dynamic of cephalopods differ for many harvested fish populations, leading to special challenges for assessing their populations and managing their fisheries[16]. Cephalopods are characterised by very fast growth rates, short life span, high fecundity, continuous spawning during a given season. In addition most cephalopods are semelparous [17], a life history where individuals reach a single, terminal reproductive event after which they die. Some cephalopods like the jumbo squid exhibit high migratory behaviour [18, 3] and age is difficult to asses given the short lifespan, with very high variability in the formation of daily increments in statolihts [19].

From an assessment viewpoint, the time-consuming nature of reading daily increments make age-based models impractical and fast and highly unequal growth rates as well as overlapping length structure of different cohorts make length-based models difficult to implement [16]. Fishery-independent surveys to assess population abundance are also impractical to be used in jumbo squid given the spatial scale of its distribution. Capture per unit of effort (CPUE) is usually used as abundance index in fisheries where fisheries-independent abundance indices are lacking. However, even the use of standardised CPUE is not recommended for highly migratory and fast-growing animals such as the jumbo squid [16]. These characteristics preclude the application of routine assessment methods usually applied in teleost

fishes which are commonly based on cohort analyses in which abundance indices are derived from surveys and/or standardised CPUE. In this context, Arkhipkin et al. [16] conducted an updated review of cephalopods stock assessment and management and recommended the use of innovative depletion models running at rapid time steps. Such family of stock assessment models do not depend on biological composition, can handle rapid life history with short life span in which ageing and fishery-independent data are not required, and natural mortality rate is estimated within the stock assessment model. Roa-Ureta et al. [20, 21, 22, 23] have presented a non-Bayesian hierarchical statistical method that combines results from generalized depletion models with generalized surplus production models to assess stocks of data-limited fisheries fisheries leading to fully analytical assessments for data-poor and data-limited fisheries. Generalized depletion models are open population models that are particularly useful in the context of the jumbo squid fishery given its trans-zonal and migratory behaviour. These depletion models are based on a mechanistic conceptualisation for the relationship between fishing effort and fish abundance as causes and fishing catch as result, thus overcoming limitations of linear approximations that use the CPUE to generate indices of relative abundance.

In addition to the challenges described above, the flying jumbo squid also show high phenotypic plasticity as a result of changes in environmental conditions [16]. Changes in the environmental conditions at the Humboldt current ecosystem (HCE) as a result of El Niño/ la Niña events have been associated with variations in growth, size at maturation and fecundity [24] and the spatio-temporal distribution of the jumbo squid [25]. Specific mechanisms on how environmental conditions are expressed in phenotypic plasticity are largely unknown, although hypotheses on how environmental temperature controlling egg size, fecundity and recruitment success have been discussed in the context of invertebrates inhabiting the HCE [26]. High phenotypic plasticity further complicates assessment and management of fishing resources because important individual attributes such as growth and fecundity will modify the productive capacity of a stock and thus resilience to fishing exploitation. In terms of fishing management, this means that biological reference points (BRP) might also change with environmental attributes. For example, Lima et al. [27] proposed that environmental cycles played a key role in the collapse of the jack mackerel at the HCE given the mismatch of managing a population with changing productivity with environment under a fixed management framework.

The main aim of this technical paper, presented to the 2023 SC SPRFMO Meeting, is to assess the jumbo squid across the SEP region using Peruvian, Asian and Chilean fleets catch, fishing effort and mean weight data at monthly time steps over the last decade (2012 to 2022), and total SEP annual landings over the last 5 decades (1969 to 20201. The model implemented is a multi-annual, 3-fleets generalised depletion model [28, 29, 20, 21, 22, 23] combined with Pella-Tomlinson surplus production model in a hierarchical non-Bayesian statistical inference method [30, 20]. At the level of the surplus production model we take into account environmental cycles caused by El niño events by estimating models with time-varying parameters.

2 Materials and Methods

2.1 FAO records of total landings

Total landings of jumbo squid in the South East Pacific by national fleet and year were extracted from the FishStatJ database version v4.03.03 (July 2023) and the last two years (2020 and 2021) were appended from database compiled in this work (Fig. 1).

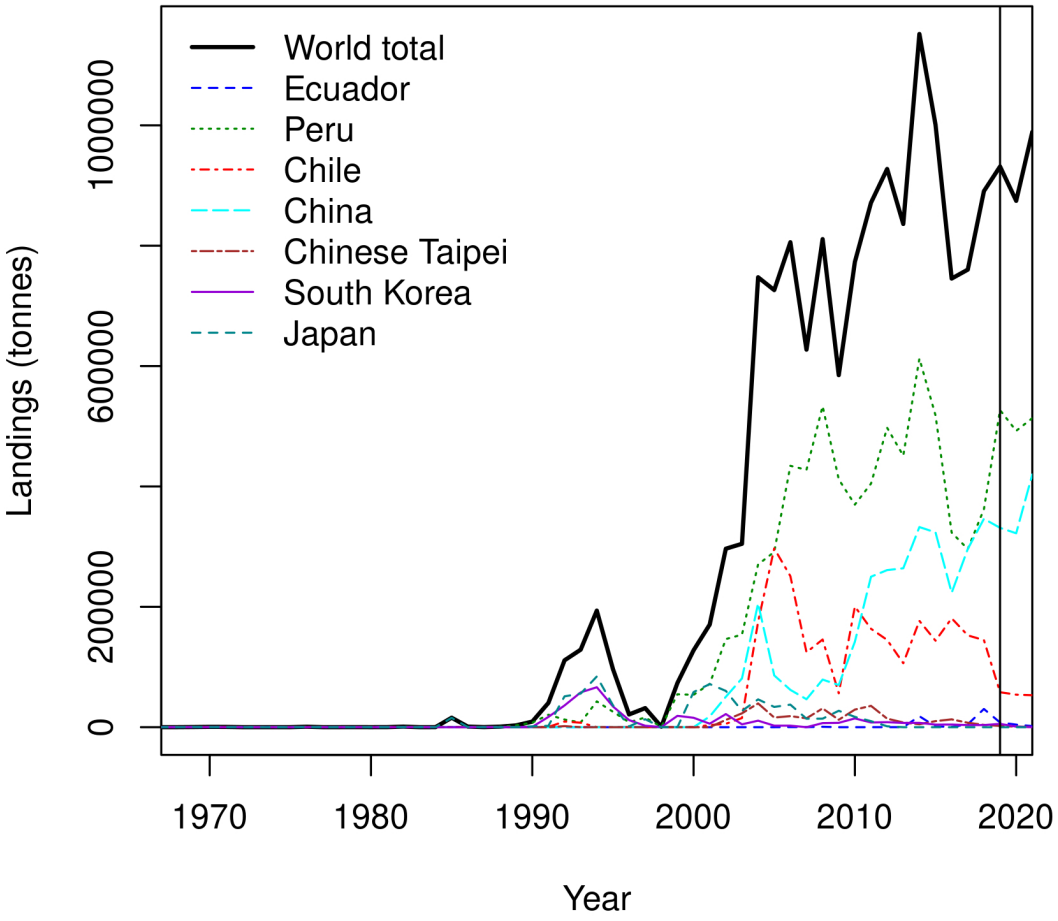

Figure 1: Time series of annual landings of jumbo squid reported by all fleets fishing in the South East Pacific from FAO databases (1969 to 2019) and data compiled from Peruvian, Chinese, South Korean, Chinese Taipei and Ecuadorian data (2020 to 2021).

Significant landings have been reported since the early 90s by Japanese, South Korean and Peruvian fleets while Chilean and Chinese fleets joined in the exploitation in the early

2000s and the Japanese fleet left operations in the early 2010s (Fig. 1). In the last decade total landings are still increasing but with substantial inter annual variability (Fig. 1).

2.2 Regional stock assessment database

The database that needs to be compiled and curated by Peruvian, Chilean, China, Chinese Taipei, South Korean and Ecuadorian fleets, to implement the multi-annual, 3-fleets generalized depletion model described in the next section, consists of total monthly landings and fishing effort, plus samples of mean weight of jumbo squids in the landings, for a number of years. The shortest database ever used to fit these models covered five years [31]. In this case, we built a 10-year catch-effort-mean weight database at monthly time steps (120 months) with Peruvian data (2012-2021) from official national sources, Chilean data (2011-2022) from official national sources, and Asian data (2012-2022) grouped for China, Chinese Taipei, and South Korea from the Scientific Committee of the South Pacific Regional Fisheries Management Organisation (SPRFMO). This database included 99.24% of all landings recorded in the region from 2012 to 2021 so our results can be safely considered as encompassing the whole stock in the SEP. Ecuadorian fleets (accounting for 0.76% of total catch between 2012 and 2021) were not included in this assessment because its database (from official national sources) was lacking in data from 2014, when fishing started in the Ecuadorian Exclusive Economic Zone, to 2017 and from September to December 2019. If the Ecuadorian database were completed we would include it despite its landings as a further, fourth separate fleet in the depletion model described in the next section.

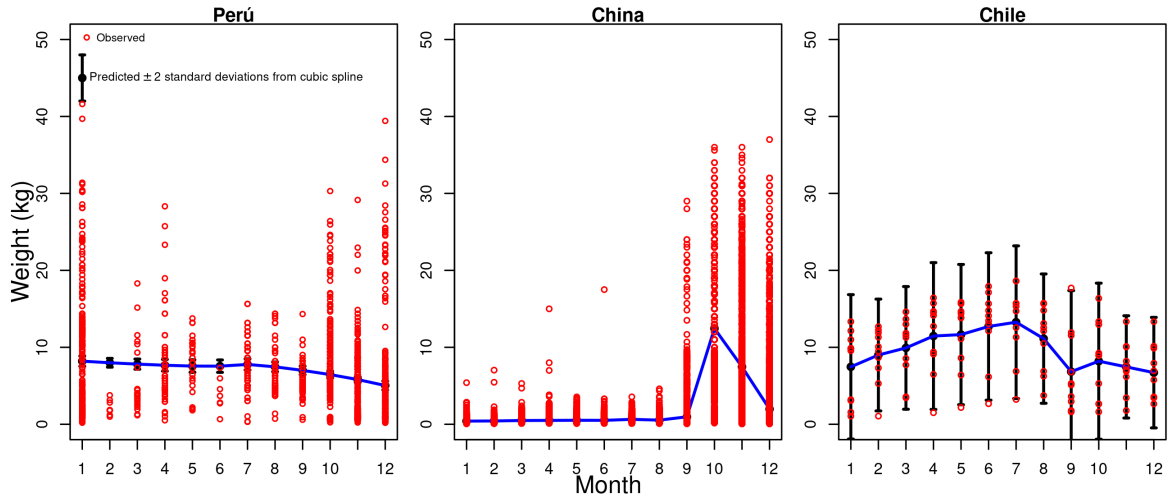

Figure 2: Raw individual jumbo squid weight data from sampling Peruvian, Chinese and Chilean data and spline model fitted to the relation between mean weight and month as well as bands of two standard errors.

The mean weight data provided is shown in Fig. 2 by month. It is clear that Chinese fleets as well as other Asian fleets operating in the high seas are harvesting smaller squids

most of the year, as described by Nigmatullin et al. [?], whereas the Peruvian and Chilean fleets catch larger squid in the waters of their Exclusive Economic Zones.

2.2.1 Peruvian fleets data

Peruvian catch-effort data from official sources covered the period from January 2012 to December 2021 in a four-column matrix of year, month, total landings in tonnes, and catch per unit of effort (CPUE) in number of squids per fishing trip, with 16 months of missing CPUE. These data presented two difficulties. First, there were 16 months of missing CPUE (14.8%, October to December 2014, September to December 2017, December 2019, January to July 2020, and November 2020) and CPUE was provided in number of squids per trip while landings were presented in tonnes, so direct solving for fishing effort in number of trips was not possible. First, we deal with the missing data problem and then with solving for fishing effort.

To predict the missing 16 months of CPUE data we used multivariate imputation chained equations with month and catch as predictors in R package **mice** [32]. The method used to impute was predictive mean matching with 1000 iterations.

To solve for fishing effort, we used the biological database provided by Peruvian official sources. The approach consisted of obtaining the monthly mean weight in the catch, multiply monthly CPUE in number of squids by the monthly mean weight in the catch to get monthly CPUE in weight per trip, and then divide the catch in weight by the CPUE in weight per trip, to solve for the monthly fishing effort vector.

Peruvian biological data were provided in two databases. One database had monthly time steps and consisted of year, month, mantle length (mm), and total individual weight (kg), from January 2012 to December 2020. A second database had annual time steps and contained the annual mean individual weight from 2000 to 2021. Calculation of the annual mean weight from the first, monthly time steps database produced substantial differences with the annual mean weights recorded in the second, annual time steps database. We assumed that the second database, built at annual time steps, had larger sample size so we conditioned the monthly mean weight from January 2012 to December 2021 obtained using the first, monthly database, to produce monthly mean weights such as the annual mean would be equal to that recorded in the second, annual time steps database. In this manner we obtained a complete vector of mean weight in the catch from January 2012 to December 2021 of the catch of the Peruvian fleet and used it to solve for monthly fishing effort in the catch and effort database.

In this manner a full database for stock assessment with multi-annual, 3-fleets generalized depletion models was completed. The mean weight data and the fitted spline model are shown in Fig. 3.

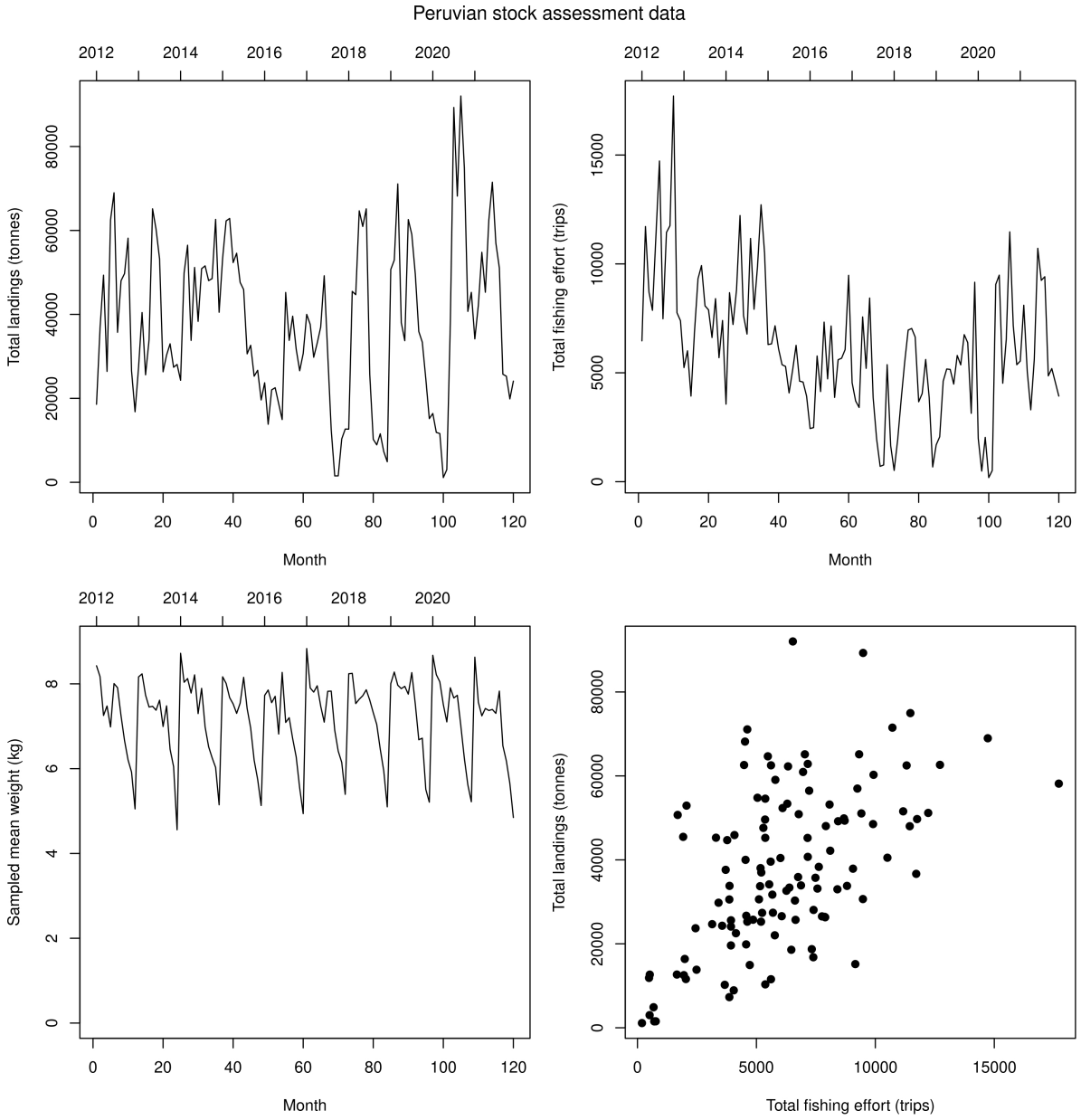

Figure 3: Time series of monthly landings, fishing effort and mean weight in the catch of Peruvian fleets fishing the jumbo squid in the South East Pacific, as well as the relation between monthly fishing effort as cause and monthly landings as result (bottom left).

2.2.2 Asian fleets data

These data were provided by the Scientific Committee of the SPRFMO (January 2012 to December 2020) and directly by China, South Korea and Taiwan (January 2021 to December 2022) and consisted in monthly catches, fishing effort, and mean location. These data were not fully dis-aggregated. Instead, individuals fishing hauls were aggregated by geographic blocks of degrees of latitude and longitude.

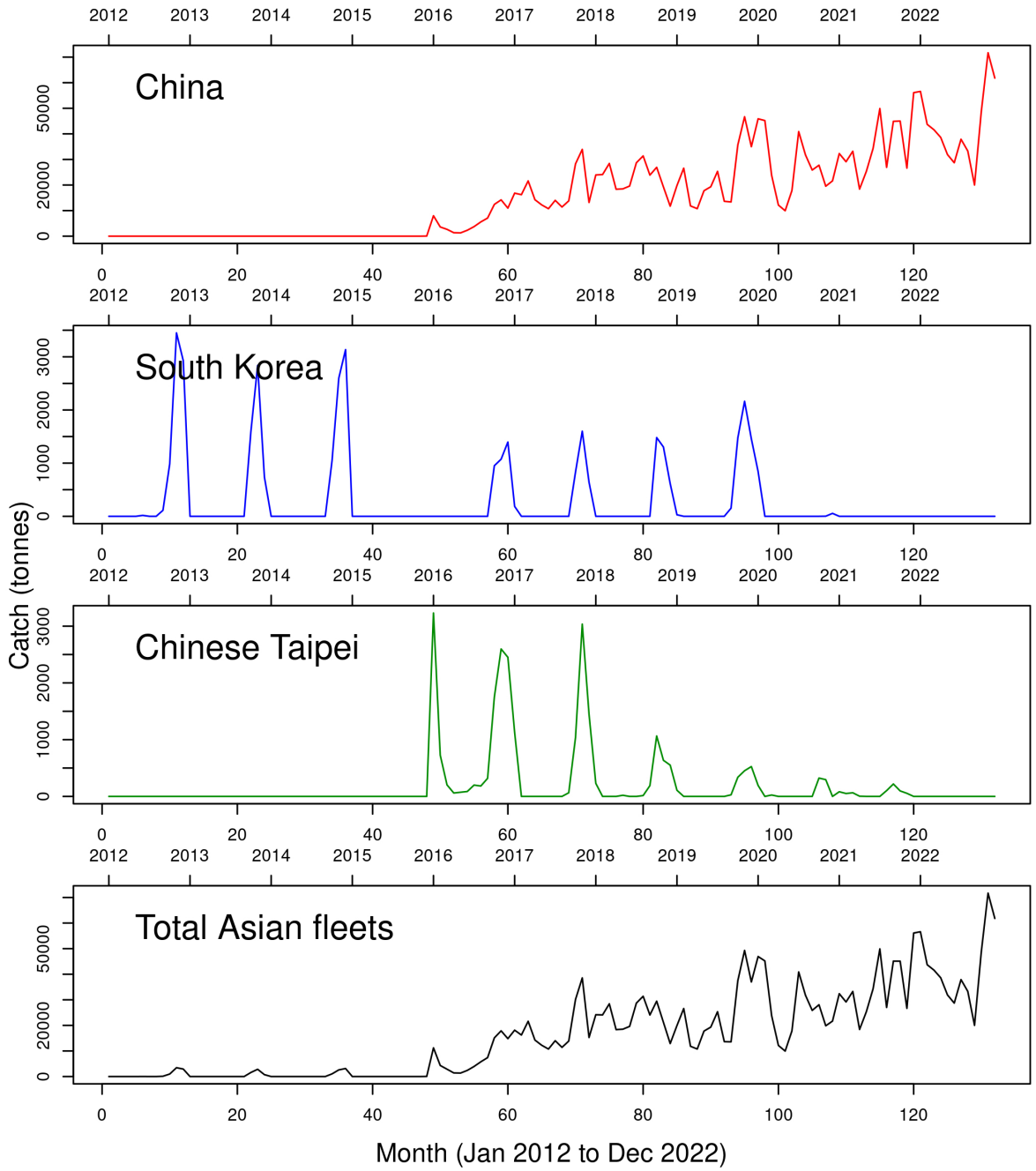

Figure 4: Time series of monthly catches reported by the three Asian fleets. Note the much larger scale of the y-axis in the China panel.

The Asian fleets database contained both, total catch in kg as well as retained and discarded catch in kg, the latter in very small quantities. In fact over 92.5% of all entries had zero discarded catch and total discarded catch accounted for 0.0013% of total catch across the time series. Nevertheless, we used the total catch (addition of retained and

discarded catch) for stock assessment purposes (Fig. 4).

The Asian fleets database included seven potential measures of fishing effort, namely the number of vessels (from a minimum of three to a maximum of 365), number of singles jigs (0 to 5,654), number of double jigs (0 to 54,235), number of jigs per line (0 to 18,351), number of hours of fishing (0 to 33,496), total power (0 to 619078 kw), number of crew (0 to 31,928) and number of days of fishing (3 to 4,397).

The Chinese fleet was the largest of the three Asian fleets by far, accounting for 2,692 of the total number of 3,181 entries in the database (over 95% of total catch), and displaying on average 1,064 vessels per month versus just 12 vessels per month in the Chinese Taipei and Korean fleets.

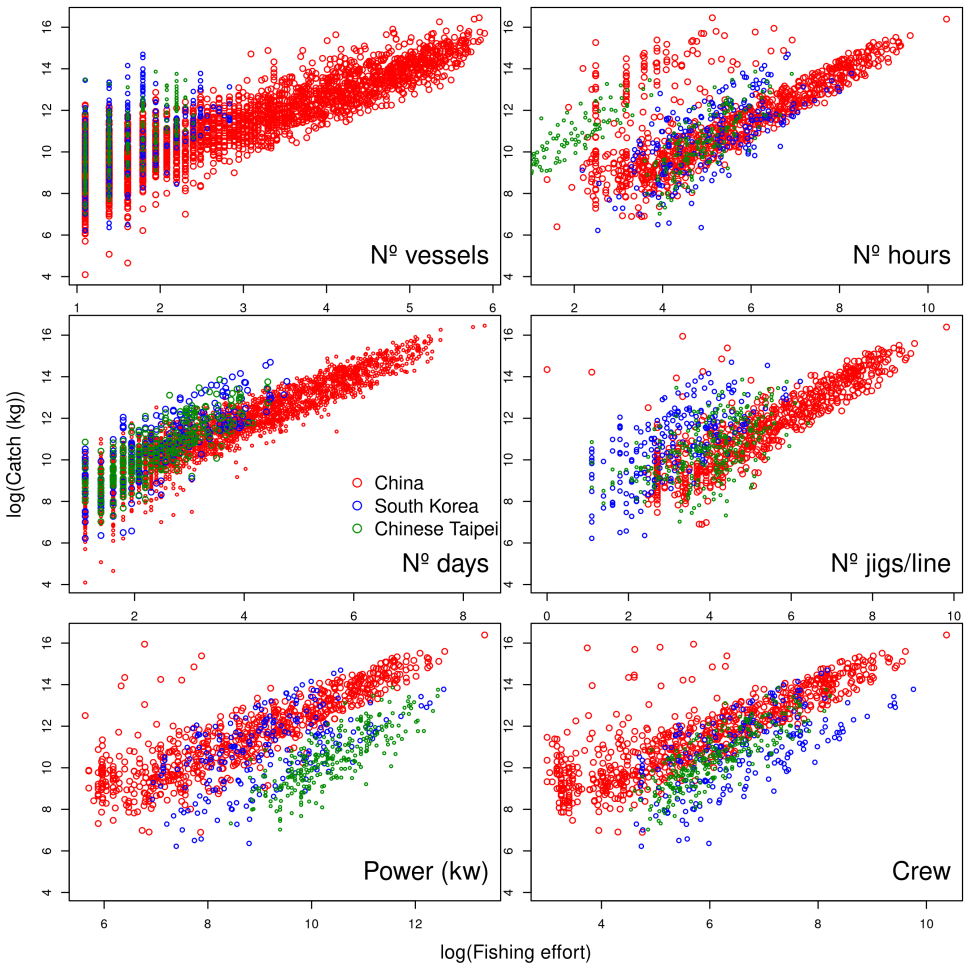

Figure 5: Catch and effort (log-log scale) of the three Asian fleets across different measurements of effort.

As stated above, the catch-effort database needs to be supplemented by a mean-weight-in-the-catch time series to apply multi-fleet multi-annual generalized depletion models. These data were kindly provided by the chairman of the jumbo squid Working Group of the

SPRFMO, Dr. Gang-Li. The data were extracted from the High Seas Observer Program of China's National Data Centre of Distant Water Fishery, and it covered the period of January 2018 to November 2021 (Fig. 2).

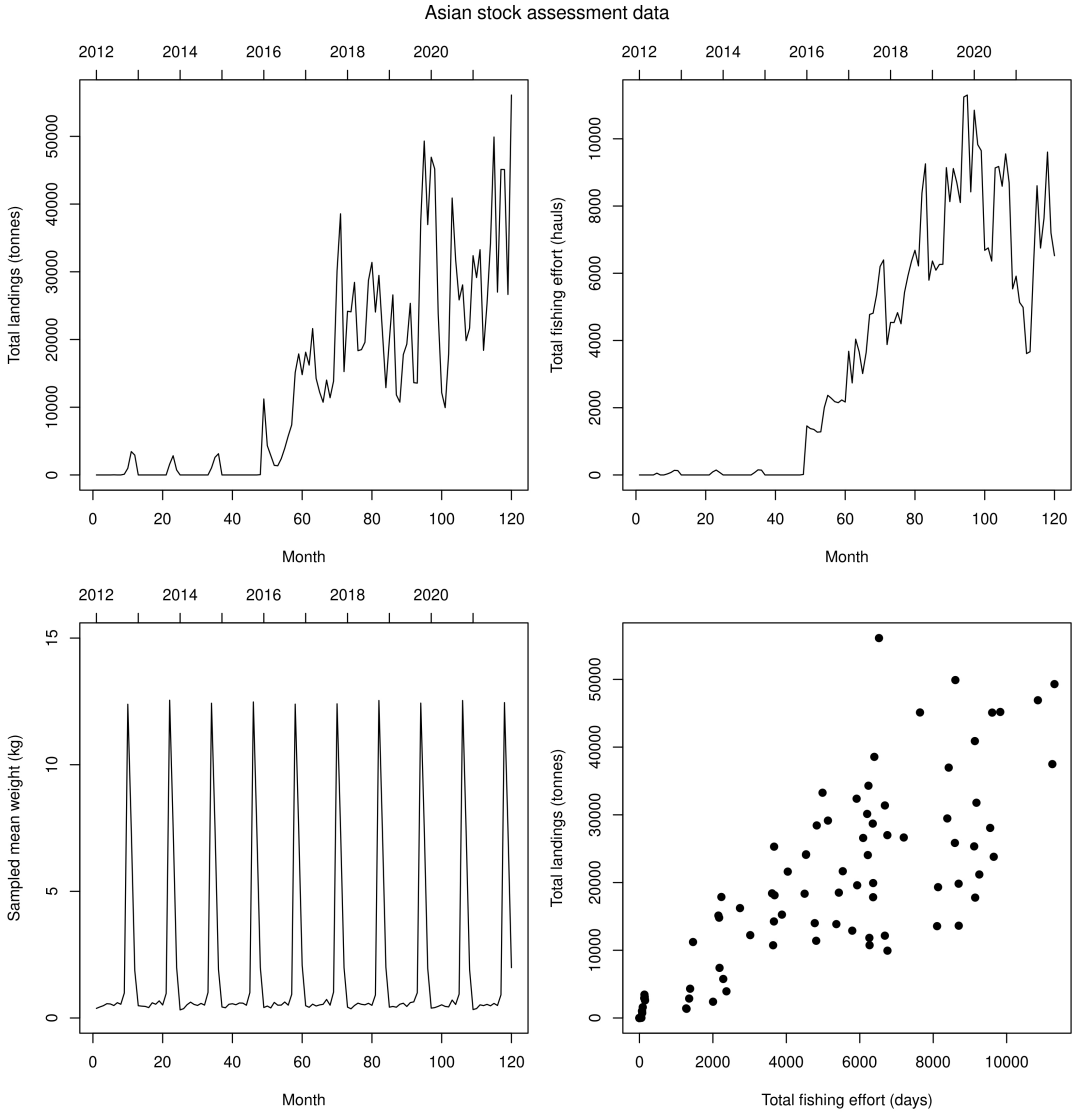

Figure 6: Time series of monthly landings, fishing effort and mean weight in the catch of Asian fleets fishing the jumbo squid in the South East Pacific, as well as the relation between monthly fishing effort as cause and monthly landings as result (bottom left).

Since Chinese squid weight data did not cover the whole period of the assessment (January 2012 to December 2021) we fitted an auxiliary model of the expected mean weight in the catch with the available data to predict mean-weight-in-the-catch for all months of the assessment database. The methodology was the same that we applied to the Peruvian biological data, namely we fitted a spline model to the relation between mean weight in the catch and month and then used its prediction along with the standard error of predictions to

populate the 108-length monthly vector of mean weight. The data and fitted spline model are shown in Fig. 2.

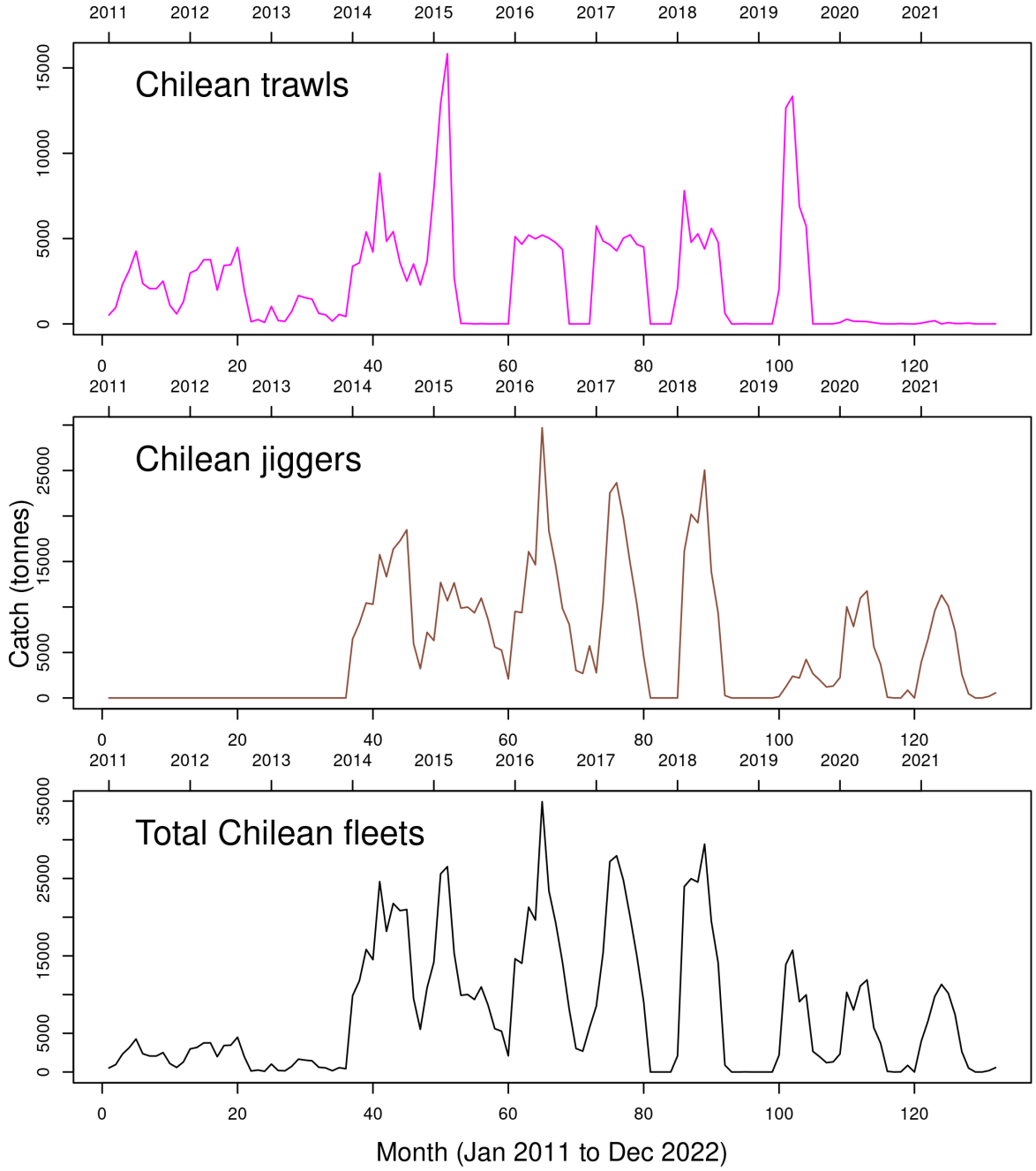

Figure 7: Time series of monthly catches reported by Chilean Fleets.

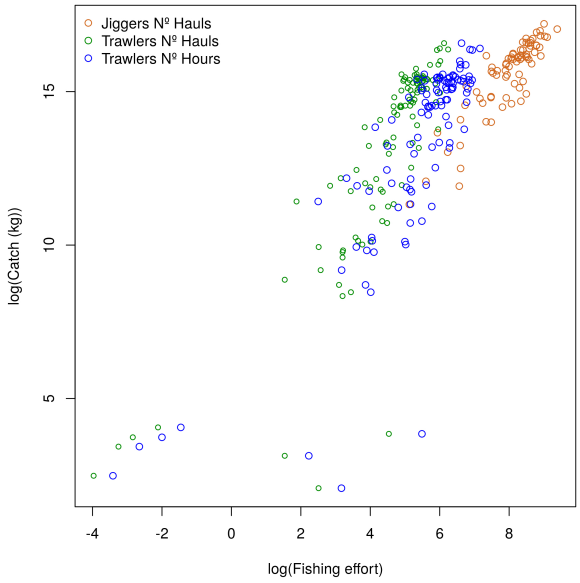

Figure 8: Catch and effort (log-log scale) of the Chilean fleets in hauls for jiggers and hauls and trawling hours trawls.

It is observed in Fig. 5 that the fishing effort metric with the tightest relation between effort as cause and catch as result and the most similar relation among China, South Korea and China Taipei is days of fishing. Therefore we selected this metric to represent fishing effort of the Asian fleets leading to a stock assessment database as shown in Fig. 6.

2.2.3 Chilean fleets data

A database of detailed logbook records from the industrial (trawlers) and artisanal (jiggers) fleets targeting jumbo squid in EEZ off Chile were provided by the Instituto de Fomento Pesquero (IFOP) upon requests directed to Chilean fishing authorities. These data consisted of dis-aggregated, haul-by-haul results of fishing for each fleet, including large samples of mantle length and whole body weight from squids in the catch, from January 2011 to December 2022 (Fig. 2). All fishing was conducted over the narrow continental shelf off central Chile inside the Chilean EEZ.

The fishing by the industrial fleet was conducted by trawling, starting in January 2011 and extending until December 2021, although it decreased substantially in 2020, to just 3.5% of the mean annual catch from 2011 to 2019, due to new legislation making the jumbo squid a resource reserved for the artisanal sector (Fig. 7). The fishing by the artisanal fleet was conducted by jigging, starting in January 2014 and extending until December 2021 (Fig. 7). Essentially, artisanal jiggers replaced industrial trawlers by legislation so there is not much utility in modelling these two fleets as separate actors. Therefore it is convenient to join the data from these two fleets and model them as a single fleet. Fortunately, Chilean databases allow calculation of additive metrics of fishing effort for the industrial and artisanal fleets when counting effort as the number of fishing hauls so this joining of the data from the two

fleets is permissible. Nevertheless, joining the effort and catch time series of the two fleets to make a single fleet further requires that the relation between effort and catch of the two fleets is not too dissimilar. Fig. 8 shows that this relation has a high similarity between the two fleets when fishing effort is measured as number of hauls. Therefore we added monthly fishing effort and monthly landings by the two fleets to have a single Chilean fleet. Since each fleet has its own mean individual weight by month, we further averaged the sampled mean weight of each fleet to get a single mean weight vector. The resulting stock assessment database of the joined Chilean fleets is shown in Fig. 9

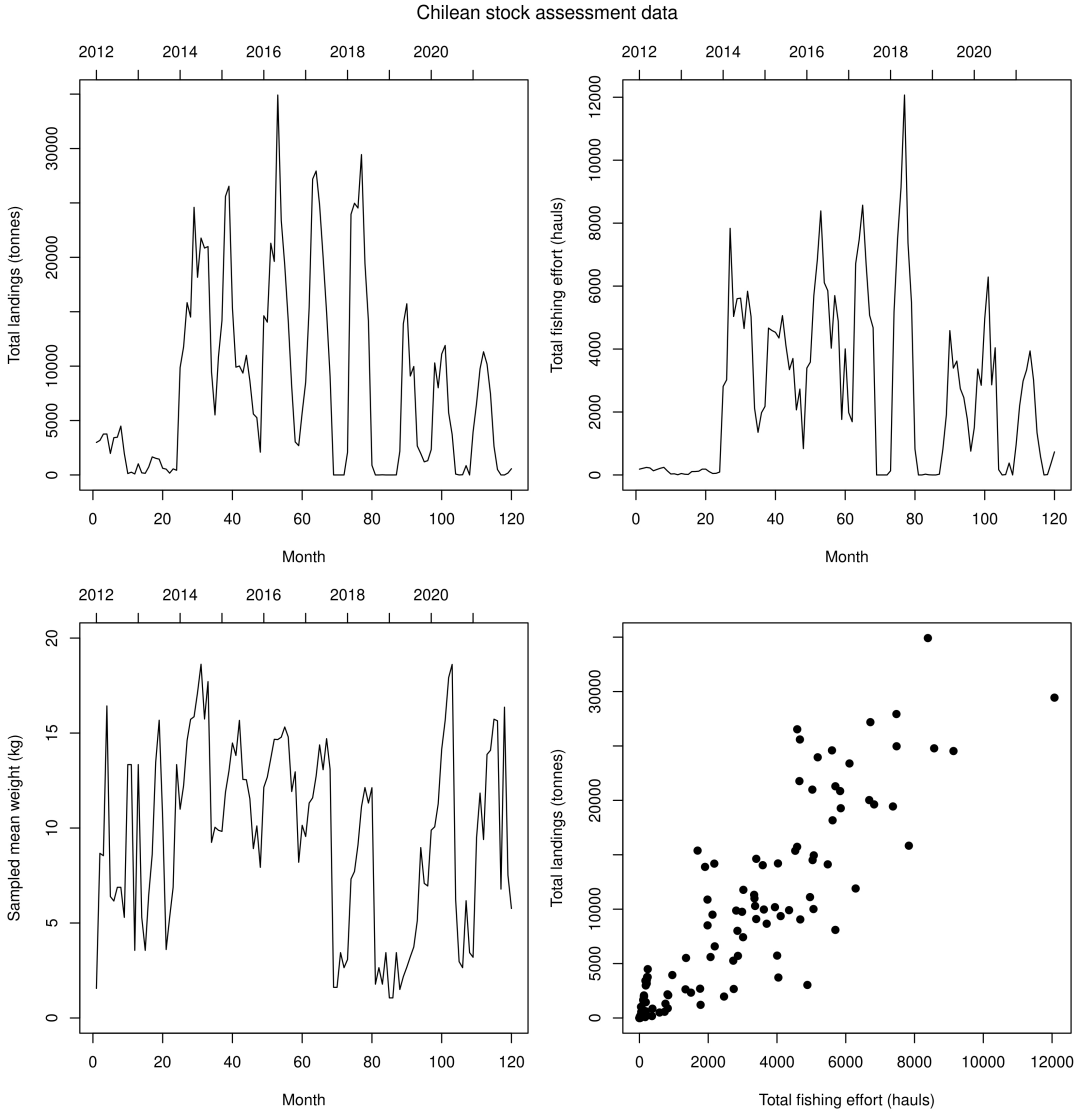

Figure 9: Time series of monthly landings, fishing effort and mean weight in the catch of Chilean fleets fishing the jumbo squid in the South East Pacific, as well as the relation between monthly fishing effort as cause and monthly landings as result (bottom left).

2.2.4 Spatial extension of Asian and Chilean fleets

Asian and Chilean data included spatial location of fishing hauls, at the individual haul level in the case of Chilean fleets and at the latitude-longitude spatial block level in the case of the Asian fleets. This allows understanding the spatial extension and expected degree of connectivity between the stock's fraction exploited by Chilean and Asian fleets.

Fig. 10 shows that Asian fleets in the SEP operate over a very large region off the Ecuadorian, Peruvian and Chilean EEZs and in international waters extending far to the west following the equatorial meridian. Catches are relatively high even at the extreme western limit of operations but most of the largest catches occur off Perú and northern Chile.

Fig. 10 also shows that Chilean fleets operate mostly in the central-south part of the country's EEZ, and that their fishing grounds are separated from Asian fleets fishing grounds by a vast extension of waters off northern Chile.

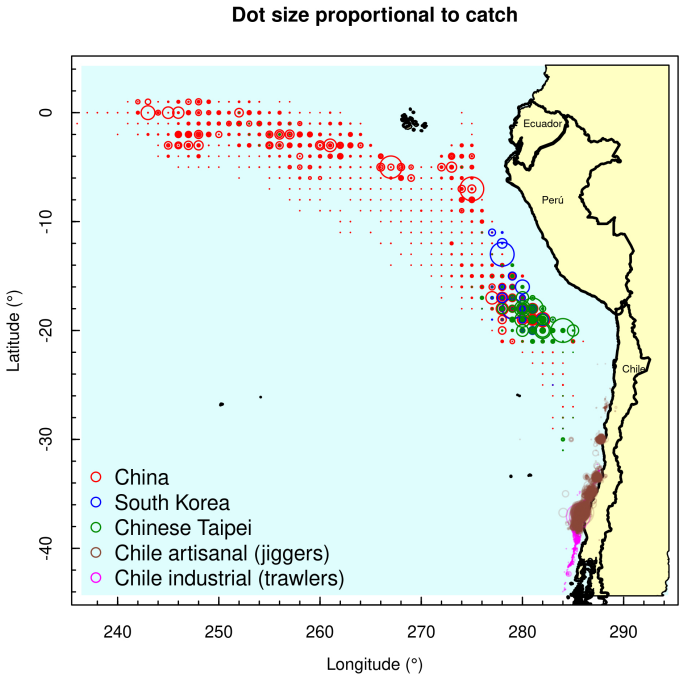

Figure 10: Spatial distribution of fishing effort by Asian and Chilean fleets.

2.3 Stock assessment methodology

The general approach to the stock assessment of the jumbo squid stock in the South-East Pacific is portrayed in schematic fashion in Fig. 10.

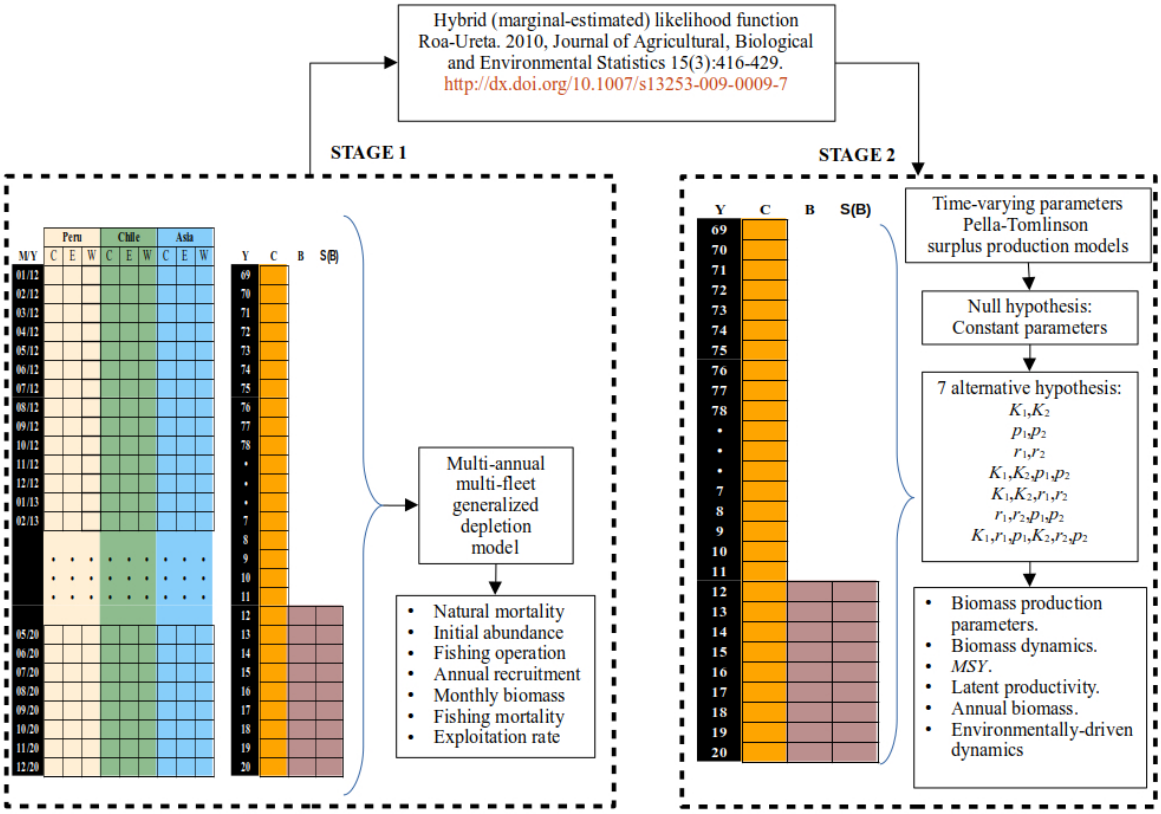

Figure 11: Schematic representation of the stock assessment modelling approach. At Stage 1, raw data of monthly catch, fishing effort and mean weight in the catch from January 2012 to December 2021 are compiled for the Peruvian, Chilean and Asian fleets. A three-fleets multi-annual generalized depletion model is fitted to these data leading to direct maximum likelihood estimates of squid abundance and fishing operational parameters and derived time series of monthly total stock abundance and biomass and fleet-specific fishing mortality and exploitation rates. A self-weighting marginal-estimated likelihood function allows the use of the biomass predicted by the depletion model and its standard error of prediction to fit a surplus production model spanning the whole period of total annual landings recorded in the FAO database (1969 to 2021). At this stage eight hypothesis are tested regarding the effect of the El Niño environmental cycle on the population dynamics and productivity of the stock.

At Stage 1, we start with landings, effort and mean weight vectors of length 108 months covering the period of January 2012 to December 2021, for three fleets. These data are used to fit multi-fleet multi-annual generalized models leading to free, unconstrained maximum likelihood estimations of the average monthly natural mortality rate from January 2012 to December 2021 (M), initial abundance (December 2011), annual recruitment to each of

the three fleets ($10 years \times 3 fleets = 30$ recruitment estimates), and three parameters of the fishing operations of each fleet, namely a generalized coefficient of catchability, a power modulator of the relation between effort as cause and catch as result, and a power modulator of the relation between abundance as cause and catch as result, totalling 38 parameters to be estimated. These are the parameters estimated directly by maximizing the log-likelihood function. In addition, results allow estimation of monthly stock's abundance and biomass, monthly fishing mortality F and monthly instantaneous exploitation rate $(M \div (M + F))$.

At Stage 2, (i) total annual landings across the SEP from 1969 to 2021 and (ii) predicted monthly biomass and its standard error from the depletion model from 2012 to 2020, are provided as information to fit a generalized surplus production model of the Pella-Tomlinson type, in order to determine population dynamics and the productivity of the stock. Assuming that at the start of the landings time series (1969) the stock's size was equal to the carrying capacity of the environment, this model has three distinct parameters. Thus, at the second stage, we consider environmental cycles due to episodic occurrences of El Niño events by testing eight alternative hypotheses of how the environmental cycle may affect the stock's population dynamics and productivity via changes in any one, any pair or all three of its parameters.

2.3.1 Generalized depletion models

Generalized depletion models are depletion models for open populations with nonlinear dynamics. Regarding the open population aspect, traditional depletion models do not admit inputs of abundance during the fishing and that is the reason they could not be used for multi-annual assessments, since in that case one obvious factor, the annual pulse of recruitment, could not be included in the assessment. Therefore, depletion models were often connected to assessing stocks with intra-annual data, for one season of fishing separately. Generalized depletion models allow any number of exogenous inputs of abundance during the fishing, so they are apt for multi-annual assessments with monthly data [29]. Regarding the nonlinear dynamics aspect, traditional depletion models assumed a linear relationship between catch as the result, and fishing effort and stock abundance as the causes of the catch. Therefore, it is common with these traditional depletion models to use the catch per unit of effort on the l.h.s of the equation and the abundance dynamics in the r.h.s. of the equation. Generalized depletion models allow for nonlinear dynamics for the effect of fishing effort and stock abundance on catch, and therefore fishing effort is not used as a standardizing quantity but as a predictor on the r.h.s. of the equation. Generalized depletion models also consider nonlinear effect of stock abundance on the resulting catch, thus taking into account phenomena such as hyper-stability [28].

With those introductory remarks, we can now define precisely the depletion model that we used to assess the jumbo squid stock in the Peruvian and Chilean EEZs and international waters. Let $C_{f,t}$ be the expected and unobserved total catch under the model from fleet f and month t and let $E_{f,t}$ be the total fishing effort from fleet f and month t. Then the model states that the total catch in month t is

$$C_t = C_{1,t} + C_{2,t} + C_{3,t} = k_1 E_{1,t}^{\alpha_1} N_t^{\beta_1} + k_2 E_{2,t}^{\alpha_2} N_t^{\beta_2} + k_3 E_{3,t}^{\alpha_3} N_t^{\beta_3}$$

$$\begin{aligned} C_t = {} & k_1 E_{1,t}^{\alpha_1} e^{M/2} \left(N_0 e^{-Mt} - e^{M/2} \left[\sum_{i=1}^{i=t-1} C_{1,i} e^{-M(t-i-1)} \right] + \sum_{j=1}^{j=9} I_{1,j} R_{1,j} e^{-M(t-\tau_{1,j})} \right)^{\beta_1} + \\ & k_2 E_{2,t}^{\alpha_2} e^{M/2} \left(N_0 e^{-Mt} - e^{M/2} \left[\sum_{i=1}^{i=t-1} C_{2,i} e^{-M(t-i-1)} \right] + \sum_{j=1}^{j=9} I_{2,j} R_{2,j} e^{-M(t-\tau_{2,j})} \right)^{\beta_2} + \\ & k_3 E_{3,t}^{\alpha_3} e^{M/2} \left(N_0 e^{-Mt} - e^{M/2} \left[\sum_{i=1}^{i=t-1} C_{3,i} e^{-M(t-i-1)} \right] + \sum_{j=1}^{j=9} I_{3,j} R_{3,j} e^{-M(t-\tau_{3,j})} \right)^{\beta_3} \end{aligned} \quad (1)$$

- t is the time step (month),
- C is the unobserved, true catch in numbers,
- k is a proportionality constant, the scaling, that corresponds to the catch taken by a unit of effort and a unit of abundance, usually in the order of 10^{-4} to 10^{-8},
- E is the observed fishing effort in hours,
- N is the latent stock abundance in numbers,
- α is a dimensionless modulator of effort as a predictor of catch, called the effort response,
- β is a dimensionless modulator of abundance as a predictor of catch, called the abundance response,
- M is the natural mortality rate with units of month^{-1},
- m equals $e^{M/2}$,
- N_0 is the initial abundance, the abundance at month before the first month in the effort and catch time series (December 2011),
- i is an index that runs over previous time steps and up to the current time step (t),
- R are the magnitudes of annual pulses (numbering 9×3) of jumbo squids that grow to the size retained by the fishers,
- I is an indicator variables that evaluates to 0 before the recruitment pulse and to 1 during and after the recruitment pulse,
- 9 is the number of recruitment pulses, one for each year, happening at a specific month each year, with j being the counter that runs from 1 to 9, and
- τ is the specific month at which each recruitment pulse happens.

In the second line of Eq. 1, latent abundance available to each fleet is made explicit and expanded with Pope's equation (second sum inside parentheses) and the input of abundance (third sum inside parentheses) corresponding to the annual recruitment (R) to the fleet in year j ($j = 1, ..., 10$, 2012 to 2021). Parameters N_0 and M are the initial abundance (December 2011) and the average (across the whole period) monthly natural mortality rate, respectively. The variable I_j is an indicator that takes the value of 0 before the input of recruitment and 1 afterwards. Finally, parameters τ_j are the months in which recruitment happens in year j.

The model in Eq. 1 is the process model, the postulated mechanism linking the true monthly catch C_t to effort and abundance, which is assumed to be fairly complete and exact, with negligible process error. The true catch time series however, are not observed. Instead, random time series $\chi_{f,t}$ are observed and its expected value is $C_{f,t}$. Thus the catch time series are random variables and the stock assessment model is completed with a statistical model with observation error where $\chi_{f,t}$ has a probability density, a specific parametric distribution. In this work, two distributions are implemented, normal and lognormal, corresponding with additive or multiplicative hypotheses for the observations of catch. In implementing the normal and lognormal distributions for the fleet's catch data, we used two likelihood functions as alternatives for each distribution, exact normal, exact lognormal, adjusted profile approximations to the normal, and adjusted profile approximations to the lognormal. The latter approximation have the following definitions:

$$l_p(\boldsymbol{\theta}; \{\chi_t, E_t\}) = \begin{cases} \frac{T-2}{2} log\left(\sum_{i=1}^{T}(\chi_t - C_t)^2\right) & Normal \\ \frac{T-2}{2} log\left(\sum_{i=1}^{T}(log(\chi_t) - log(C_t))^2\right) & Lognormal \end{cases} \quad (2)$$

where l_p is the negative log-likelihood function, $\boldsymbol{\theta}$ is the vector of parameters, $\{\chi_t, E_t\}$ are the catch and effort data, C_t is the predicted catch according to the model in Eq. 1, and T is the total number of months ($T = 108$ with nine years of data). These negative log-likelihood functions are minimized numerically as a function of $\boldsymbol{\theta}$ to estimate maximum likelihood parameter values and their covariance matrix. The $38 + \times 38+$ covariance matrix contains the asymptotic standard errors of parameter estimates along its main diagonal and the co-variances or correlations in the off diagonal triangles.

The model has 41 differentiable parameters (N_0, M, $\{R_{i,j}\}$, k_1, k_2, k_3, α_1, α_2, α_3, β_1, β_2, β_3) and 30 non-differentiable parameters ($\{\tau_{f,j}\}$), the latter corresponding to the month of recruitment in each year to each fleet, which we call the timing for short. The $\{\tau_{f,j}\}$ can be determined by setting the input of recruitment at the month within a year with the lowest mean weight, because recruitment is assumed to happen due to somatic growth of small squids reaching the sizes captured and retained by fishers, so it should be noticeable by observing the lowest mean weight of squid in the catch. The timing can further be determined by recourse to the non-parametric catch spike statistics [29],

$$Spike_t = 10\left(\frac{\chi_t}{max(\chi_t)} - \frac{E_t}{max(E_t)}\right) \quad (3)$$

where χ is the observed catch. It highlights time steps with excessively high catch for the

effort at that time step, thus suggesting a recruitment input whenever the spike is large and positive. See Fig. 3 in Roa-Ureta et al. [23] for a graphical demonstration of the use the spike statistic.

After examination of optimization results with the initial timing hypothesis, the inability of optimization routines to calculate the standard error of recruitment magnitudes, or calculating very large standard errors for some recruitment magnitudes, suggest the need to set the month of recruitment in those year and fleet combinations in different months, so further hypotheses were evaluated by changing the months of recruitment for some years.

The four likelihood functions (adjusted profile normal, adjusted profile lognormal, exact normal, and exact lognormal) can be applied individually to each of the three fleets so there are a total of $4^3 = 64$ full combined likelihoods. In addition, the different timing hypotheses create further options each one to be fitted under each of the 64 full combined likelihoods. Furthermore, we employed three different numerical maximization methods in R, namely the *spg*, *CG*, and *Nelder-Mead* methods for likelihood optimization because these have yielded reliable results in previous applications [23, 33, 34]. Therefore, dozens of variants of the model in Eq. 1 were fitted to the data of the three fleets. The final best variant was selected as the one with better numerical, biological and statistical quality criteria. Firstly, all fits returning a numerical gradient higher than 1 were eliminated. This is a commonly employed criterion in stock assessment [35, 36, 37, 38]. Secondly, variants yielding unrealistic values of the natural mortality rate (i.e. less than 0.01 per month) were also excluded, given the known short lifespan of the jumbo squid. Thirdly, from the short list of model fits, the best fit was selected as the one with the lowest standard errors and with the histogram of correlation coefficients between parameter estimates more concentrated around zero. The histogram of correlation coefficients presents the distribution of pairwise correlations between parameter estimates. It is desirable that these correlations are as far away from 1 or -1 as possible because that means that each parameter was a necessary component of the model. Information theory model selection methods such as the Akaike Information Criterion (AIC) are also useful at this stage when comparing models run with the same likelihood or approximation to the likelihood.

Generalized depletion models were fitted using a customized version of R package CatDyn [34]. All parameters were freely estimated, none of them was fixed at arbitrary values. CatDyn also estimates fishing mortality per month using a numerical resolution (R function *uniroot*) of the Baranov equation from estimates of abundance, natural mortality and (observed and estimated) catch per month. CatDyn depends on package optimx [39], which makes it simple to call several numerical optimization routines as alternatives to minimize the negative log-likelihood.

2.3.2 Population dynamics models

Generalized depletion models estimate abundance at the start of the time series in the N_0 parameter. Abundance then drops due to natural mortality and fishing removals and is reset to a higher value with every input of abundance due to recruitment, one for each year and fleets in the time series. Therefore, for each year, total abundance (initial abundance plus recruitment inputs) at all time steps (108 months) can be obtained by rolling back

recruitment pulses from the month of recruitment and adding that to initial abundance decaying through natural mortality. Rolling back entails using the natural mortality rate estimate M with reversed sign. Knowing also the mean weight per month monthly abundance can be transformed into biomass, B_t. In addition, statistical uncertainty is propagated from initial abundance, natural mortality, and recruitment estimates and their covariance matrix, to each monthly total abundance using the delta method. This leads to time series of total monthly abundance and its standard error. Furthermore, total biomass at each time step B_t is estimated with its standard error using the total abundance estimate and its standard error and the mean weight in the catch per month and its standard error, with additional use of the delta method. The function *CatDynBSD* in CatDyn does this calculation to propagate statistical uncertainty in N_0, M, the $\{R_{f,j}\}$ and mean weight, to B_t.

The estimated biomass time series and its standard error extends at monthly time steps over the complete time series. As it happens, it is often the case that a particular month produces the biomass estimate with the lowest standard error inside each year. We evaluate this month as the month at which the mean coefficient of variation (CV) of the biomass estimate is the lowest on average across the years. The main purpose of using a particular month of biomass estimate from each year is to have an annual time step in the surplus production model. Having an annual time step is convenient because it is possible to use the landings from years prior to the year of the first biomass estimate with CatDyn, as additional data to fit the surplus production model. Selecting the month with the least average (across years) CV of the biomass estimate helps have more precise estimates of parameters in the surplus production model.

The South-East Pacific region is affected by the periodic occurrence of the El Niño Southern Oscillations (ENSO) leading to multi-annual periods of increased water temperature followed by multi-annual periods of colder or normal temperature [40]. These environmental oscillations may well affect the stock's population dynamics. We used NOAA's ENSO index [41] to define six environmental phases during our study period:

1. 1969 to 1981: Normal or cold period 1
2. 1982 to 1988: El Niño 1
3. 1989 to 1996: Normal or cold period 2
4. 1997 to 2002: El Niño 2
5. 2003 to 2013: Normal or cold period 3
6. 2014 to 2021: El Niño 3

Then we defined eight hypotheses of biomass dynamics during the study period (Fig. 12). The first hypothesis was the null hypothesis that the biomass dynamics was a conventional Pella-Tomlinson dynamics with constant parameters during the whole study period (1969 to 2021), i.e.:

$$B_y = B_{y-1} + rB_{y-1}\left(1 - \left(\frac{B_{y-1}}{K}\right)^{p-1}\right) - C_{y-1}, p > 1, 1969 \leq y \leq 2020 \tag{4}$$

where

- y is the year,
- r is the intrinsic population growth rate,
- p is the symmetry of the production function,
- K is the carrying capacity of the environment,
- B_y is the biomass estimated from generalized depletion models, and
- C_{y-1} is the total regional annual catch during the previous fishing season,

The seven alternative hypotheses were that the biomass dynamics, i.e. the Pella-Tomlinson model, had time-varying parameters that followed the environmental cycle:

$$\begin{aligned}
B_y &= B_{y-1} + r_1 B_{y-1}\left(1 - \left(\frac{B_{y-1}}{K_1}\right)^{p_1-1}\right) - C_{y-1}, p_1 > 1, 1969 \leq y < 1982 \\
B_y &= B_{y-1} + r_2 B_{y-1}\left(1 - \left(\frac{B_{y-1}}{K_2}\right)^{p_2-1}\right) - C_{y-1}, p_2 > 1, 1982 \leq y < 1989 \\
B_y &= B_{y-1} + r_1 B_{y-1}\left(1 - \left(\frac{B_{y-1}}{K_1}\right)^{p_1-1}\right) - C_{y-1}, p_1 > 1, 1989 \leq y < 1997 \\
B_y &= B_{y-1} + r_2 B_{y-1}\left(1 - \left(\frac{B_{y-1}}{K_2}\right)^{p_2-1}\right) - C_{y-1}, p_2 > 1, 1997 \leq y < 2002 \\
B_y &= B_{y-1} + r_1 B_{y-1}\left(1 - \left(\frac{B_{y-1}}{K_1}\right)^{p_1-1}\right) - C_{y-1}, p_1 > 1, 2002 \leq y < 2014 \\
B_y &= B_{y-1} + r_2 B_{y-1}\left(1 - \left(\frac{B_{y-1}}{K_2}\right)^{p_2-1}\right) - C_{y-1}, p_2 > 1, 2014 \leq y < 2021
\end{aligned} \tag{5}$$

so the full set of hypotheses is defined by

- Null hypothesis: $K_1 = K_2, p_1 = p_2, r_1 = r_2$ (Eq. 4),
- Alternative 1: $K_1 \neq K_2, p_1 = p_2, r_1 = r_2$ (Eq. 5),
- Alternative 2: $K_1 = K_2, p_1 \neq p_2, r_1 = r_2$ (Eq. 5),
- Alternative 3: $K_1 = K_2, p_1 = p_2, r_1 \neq r_2$ (Eq. 5),

- Alternative 4: $K_1 \neq K_2, p_1 \neq p_2, r_1 = r_2$ (Eq. 5),
- Alternative 5: $K_1 \neq K_2, p_1 = p_2, r_1 \neq r_2$ (Eq. 5),
- Alternative 6: $K_1 = K_2, p_1 \neq p_2, r_1 \neq r_2$ (Eq. 5),
- Alternative 7: $K_1 \neq K_2, p_1 \neq p_2, r_1 \neq r_2$ (Eq. 5).

So alternative hypotheses described increasingly complex changes in parameter values as the environmental cycle developed. The most supported hypothesis was selected considering numerical, statistical and biological criteria as described for model variant selection at Stage 1, except that in this model selection task the AIC plays a more prominent role because all hypotheses are fitted with the same likelihood function.

Total regional annual biomass and its standard error from fitting generalized depletion models and the annual biomass predicted by alternative hypotheses of time-varying parameters of the Pella-Tomlinson model are linked through a hybrid (marginal-estimated) likelihood function,

$$\ell_{HL}(\boldsymbol{\theta}_{PT}|\{\hat{B}_y\}) \propto -\frac{1}{2}\sum_{2012}^{2020}\left(log(2\pi S^2_{\hat{B}_y}) + \frac{(\hat{B}_y - B_y)^2}{S^2_{\hat{B}_y}}\right) \tag{6}$$

where

- $\boldsymbol{\theta} = \{K, r, p\}$ is the vector of parameters of the Pella-Tomlinson model in Eq. 4 or 5. In all hypotheses it is assumed that the biomass in the first year in the landing time series, 2012, is equal to the carrying capacity of the environment (initial probes with the null hypothesis model and B_0 as additional parameter did not yield successful convergence),
- $S^2_{\hat{B}_y}$ are the distinct numerical estimates of standard deviations of each annual biomass estimate from the fitted generalized depletion model (replacing the unknown distinct true standard deviations),
- $\hat{B}_y$ are the maximum likelihood estimates of annual biomass from the fitted generalized depletion model, and
- B_y are the true annual biomass according to Eq. 4 or 5.

The log-likelihood function in Eq. 6 is self-weighting in the sense of Francis [42, 43], meaning that it automatically up-weights annual biomass estimates with higher statistical precision and down-weights annual biomass estimates with lower statistical precision during likelihood optimization.

From the fit of best-supported hypothesis Pella-Tomlinson model, several biological reference points were calculated. The reference points were the MSY,

$$MSY = rK(p-1)p^{-p/(p-1)} \tag{7}$$

the biomass at the MSY,

$$B_{MSY} = Kp^{1/(1-p)} \tag{8}$$

and the latent productivity,

$$\dot{P} = \gamma MSY \frac{B_y}{K}\left(1 - \left(\frac{B_y}{K}\right)^{p-1}\right), \gamma = \frac{p^{p/(p-1}}{p-1} \tag{9}$$

For each biological reference points, standard errors were computed using the delta method whenever possible.

With reference to the latent productivity [44], this is a biological reference point analogous to the MSY, but while MSY is a constant, the latent productivity varies with the biomass of the stock (compare Eq. 7 to Eq. 9). Thus the latent productivity is more relevant for stocks that tend to fluctuate because of environmental forces or because of their intrinsic population dynamics. For instance, in [20] we found that the stock under study was fluctuating because of a high value of the intrinsic population growth rate, r. In another case [23] we found that the stock was undergoing cyclic fluctuations due to an unstable equilibrium point in the spawners-recruitment relationship. Thus the MSY was not applicable in those cases and it was actually an excessive harvest rate.

The analysis at this stage was programmed in ADMB [45] using ADMB-IDE 10.1 64 bits [46]. We created ADMB code for each of the eight environmental influence hypotheses. Taking advantage of facilities of the ADMB system, parameter estimation was carried out by bounded or unbounded optimization, depending on the parameter and the model variant, and the *sdreport* function was used to produce annual biomass estimates with their standard errors.

3 Results

3.1 Generalized depletion models

The selected variant of the depletion model was conducted with a joint likelihood that combined the adjusted profile lognormal likelihood for the Peruvian catch data, the adjusted profile lognormal likelihood for the Chilean catch data, the adjusted profile normal likelihood for the Asian catch data, and the *spg* numerical method. The fit of this variant to data is shown in Figs. 12, 13, and 14.

The model fits the Peruvian monthly catch data data well, with adequate residual and quantile diagnostics (Fig. 12). It fits the Asian catch data less well, failing to predict high catches in the last two years (2020, 2021) and having a q-q plot with observed quantiles falling below the diagonal (Fig. 13). The model fits the Chilean catch data very well, with just two observed monthly catches bot falling on the diagonal on the q-q plot (Fig. 14). Escapement biomass (December 2021) at the regional level is estimated at 2.5 million tonnes

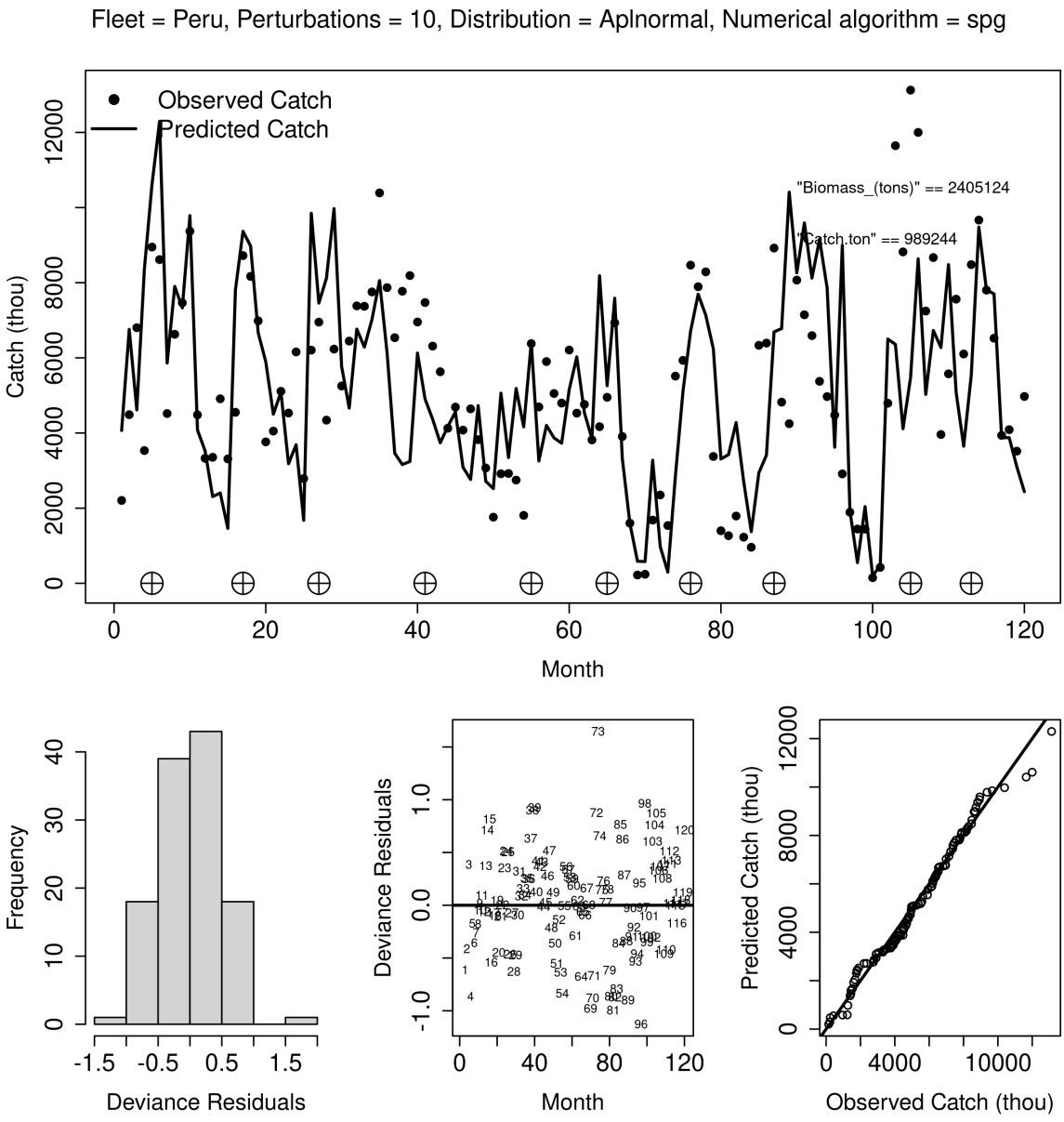

Figure 12: Fit of the depletion model to catch in numbers data from Peruvian fleets operating on the fishery for the jumbo squid in the Peruvian EEZ of the SEP. Top panel: Model fit to data also indicating timing of recruitment inputs (target symbol), escapement biomass, and annual catch. Bottom panels, from left to right: histogram of residuals, residual cloud, and q-q plot.

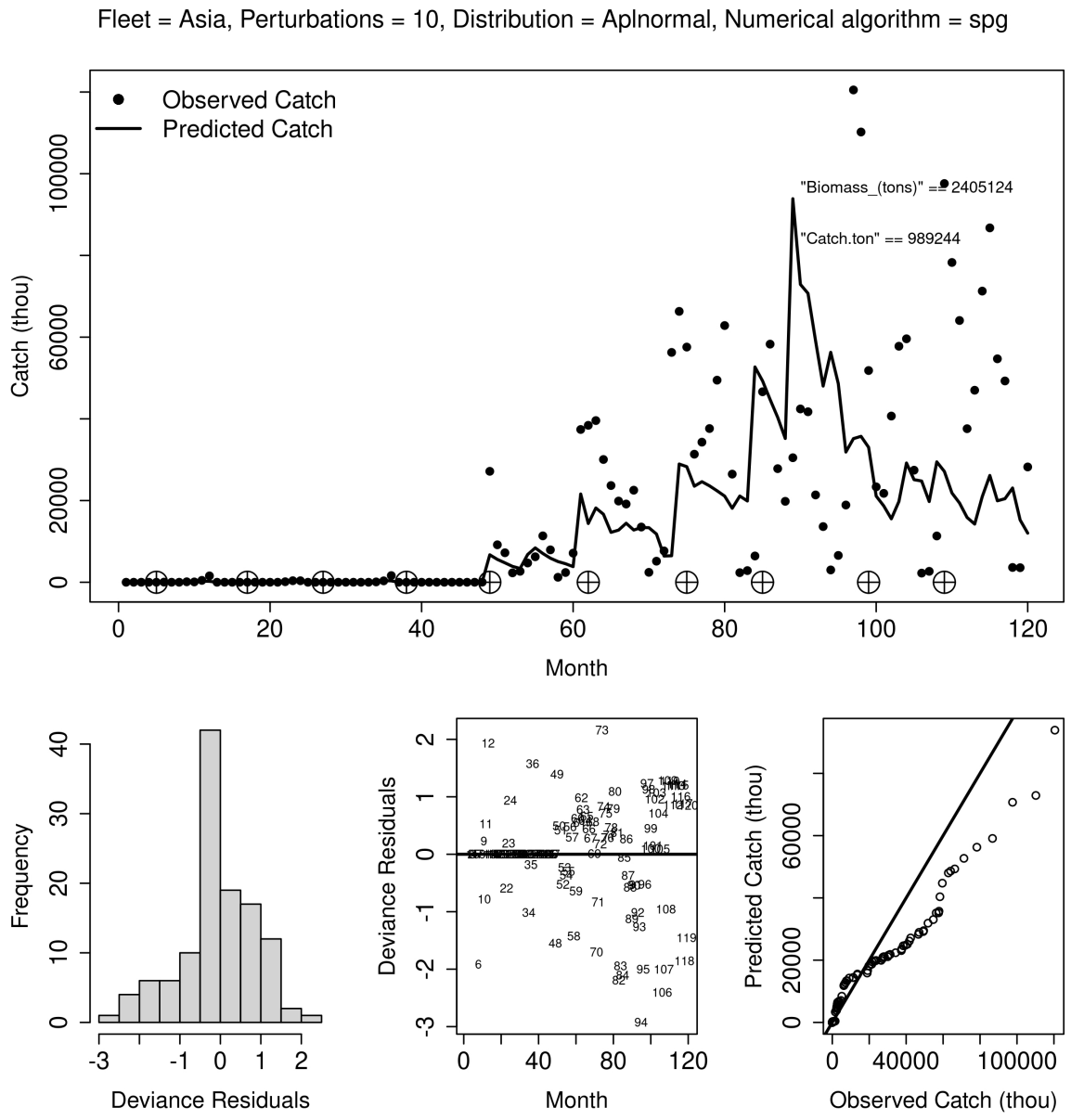

Figure 13: Fit of the depletion model to catch in numbers data from Chilean fleets operating on the fishery for the jumbo squid in the Chilean EEZ of the SEP. Top panel: Model fit to data also indicating timing of recruitment inputs (target symbol), escapement biomass, and annual catch. Bottom panels, from left to right: histogram of residuals, residual cloud, and q-q plot.

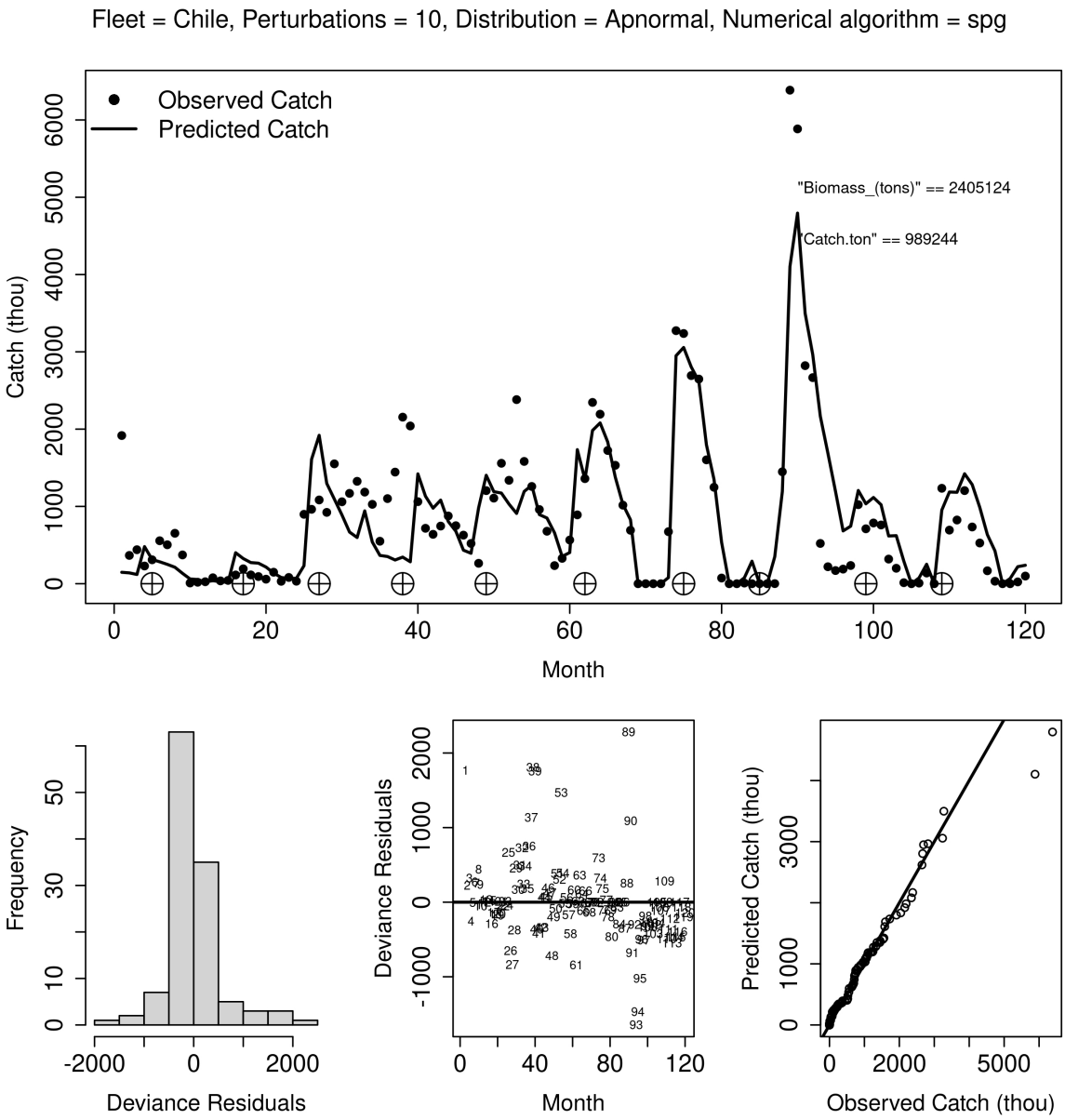

Figure 14: Fit of the depletion model to catch in numbers data from Asian fleets operating on the fishery for the jumbo squid in international waters of the SEP. Top panel: Model fit to data also indicating timing of recruitment inputs (target symbol), escapement biomass, and annual catch. Bottom panels, from left to right: histogram of residuals, residual cloud, and q-q plot.

Table 1: Maximum likelihood parameter estimates of the best 3-fleets multi-annual generalized depletion models. Absent CVs: the optimizer did not return standard errors.

Fleet	**Parameter**	**Timing**	**Estimate**	**CV** (%)
	M (1/month)		0.1611	12.3
	N_0 (thousand)		715,637	29.2
Peruvian fleets	Recruitment (thousand) 2012	2012-5	1,100,637	27.70
	Recruitment (thousand) 2013	2013-5	1,466,690	40.60
	Recruitment (thousand) 2014	2014-3	1,387,826	22.10
	Recruitment (thousand) 2015	2015-4	1,050,525	28.60
	Recruitment (thousand) 2016	2016-6	414,176	164.70
	Recruitment (thousand) 2017	2017-5	198,056	165.40
	Recruitment (thousand) 2018	2018-3	80,338	169.30
	Recruitment (thousand) 2019	2019-3	213,686	
	Recruitment (thousand) 2020	2020-9	415,839	101.20
	Recruitment (thousand) 2021	2021-4	285,622	95.90
	k (1/trips)		0.00015347	43.3
	α		0.9447	9.0
	β		0.6670	6.1
Asian fleets	Recruitment (thousand) 2012	2012-5	6,802	
	Recruitment (thousand) 2013	2013-5	8,779	
	Recruitment (thousand) 2014	2014-3	8,856	
	Recruitment (thousand) 2015	2015-1	7,388	
	Recruitment (thousand) 2016	2016-12	1,254,228	24.1
	Recruitment (thousand) 2017	2017-2	1,607,369	18.3
	Recruitment (thousand) 2018	2018-3	1,860,553	21.3
	Recruitment (thousand) 2019	2019-12	2,756,364	14.0
	Recruitment (thousand) 2020	2020-3	199,125	137.9
	Recruitment (thousand) 2021	2021-1	1,244,206	36.4
	k (1/days)		0.000009393	348.8
	α		0.9305	8.0
	β		0.9714	26.8
Chilean fleets	Recruitment (thousand) 2012	2012-1	64,232	
	Recruitment (thousand) 2013	2013-3	5,687	
	Recruitment (thousand) 2014	2014-10	419,915	
	Recruitment (thousand) 2015	2015-7	304,531	134.5
	Recruitment (thousand) 2016	2016-8	235,101	294.9
	Recruitment (thousand) 2017	2017-9	63,776	365.0
	Recruitment (thousand) 2018	2018-9	6,326	390.9
	Recruitment (thousand) 2019	2019-6	2,212,205	28.8
	Recruitment (thousand) 2020	2020-9	25,121	
	Recruitment (thousand) 2021	2021-9	16,064	
	k (1/hauls)		0.0000002297	7.4
	α		0.4088	16.0
	β		1.3687	0.6

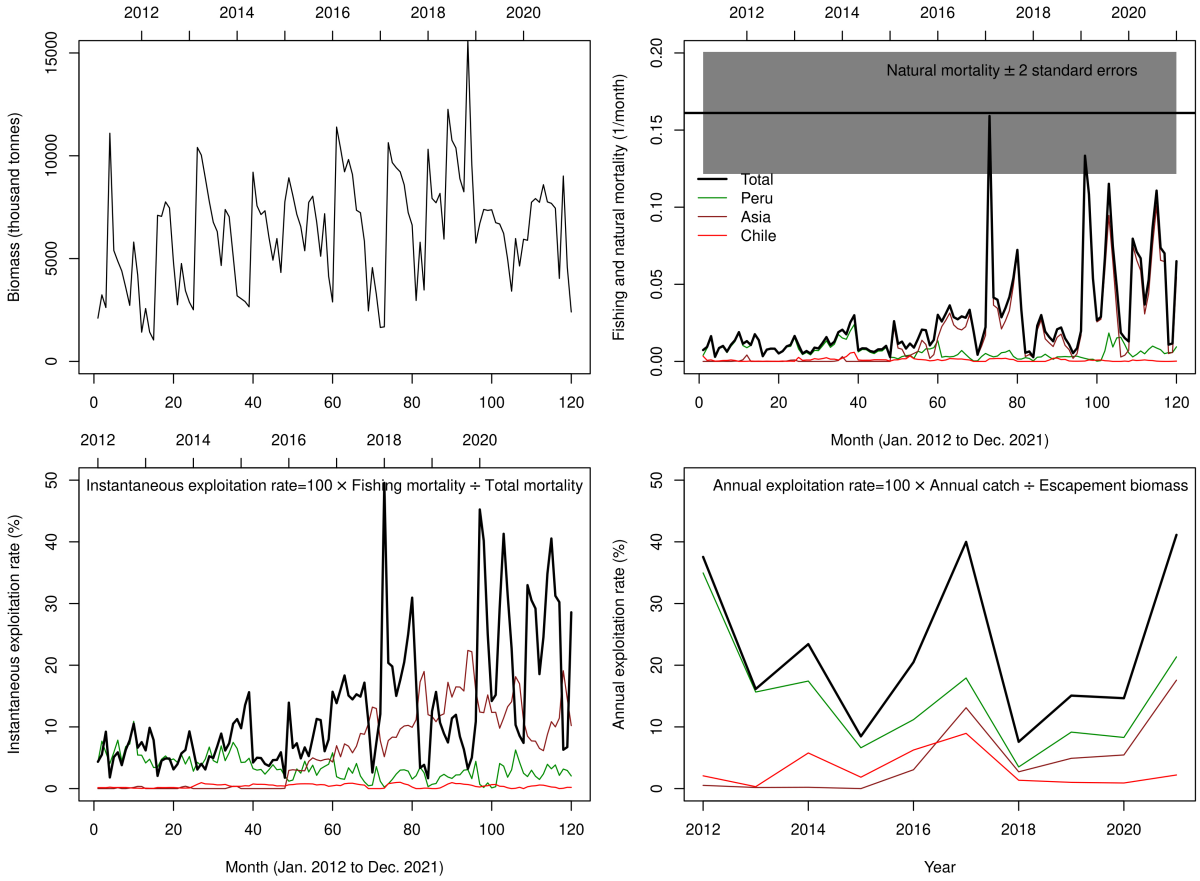

Figure 15: Time series of interest in management. Top left: stok biomass; top right: fishing and natural mortality; bottom left: instantaneous exploitation rate; bottom right: annual exploitation rate with respect to escapement biomass

Estimated parameters by the selected depletion model for the three fleets data are shown in Table 1. Natural mortality is estimated at 0.1611 per month or 1.9332 per year, with good statistical precision. Abundance parameters (N_0 and recruitment) are generally estimated with good precision but there are many missing standard errors, a consequence of difficult optimization over some of the 41 dimensions of the problem with R optimization routines. Recruitment has been decreasing for the Peruvian fleets, increased substantially for the Asian fleets, and fluctuating widely for the Chilean fleets. The response of catch to effort is close to proportional for the Peruvian and Asian fleets and saturable for the Chilean fleets while the response to abundance is hyper-stable for Peruvian, proportional for Asian, and slightly hyper-depleted for Chilean fleets.

Derived parameters from the best supported depletion model are shown in Fig. 15. Biomass has wide intra-annual fluctuations, with maxima one order of magnitude larger than minima, and the mean trend has been gradually increasing up to 2019 and then decreasing in 2020 and 2021. Fishing mortality has been much lower than natural mortality but it has increased in recent years, approaching the level of natural mortality, and the same increasing trend is observed in the instantaneous exploitation rate. Finally the annually aggregated

exploitation rate with respect to escapement biomass shows is W-shaped, with recent raise due to lower biomass. Nevertheless, both the instantaneous and the aggregated exploitation rate are yet not above 40%. Therefore fishing mortality and total removals appear to be still within safe limits.

Calculation of standard errors of abundance and biomass time series with the delta method results in estimates that are reasonably precise (Fig. **??**). This will have a positive effect on inference at Stage 2.

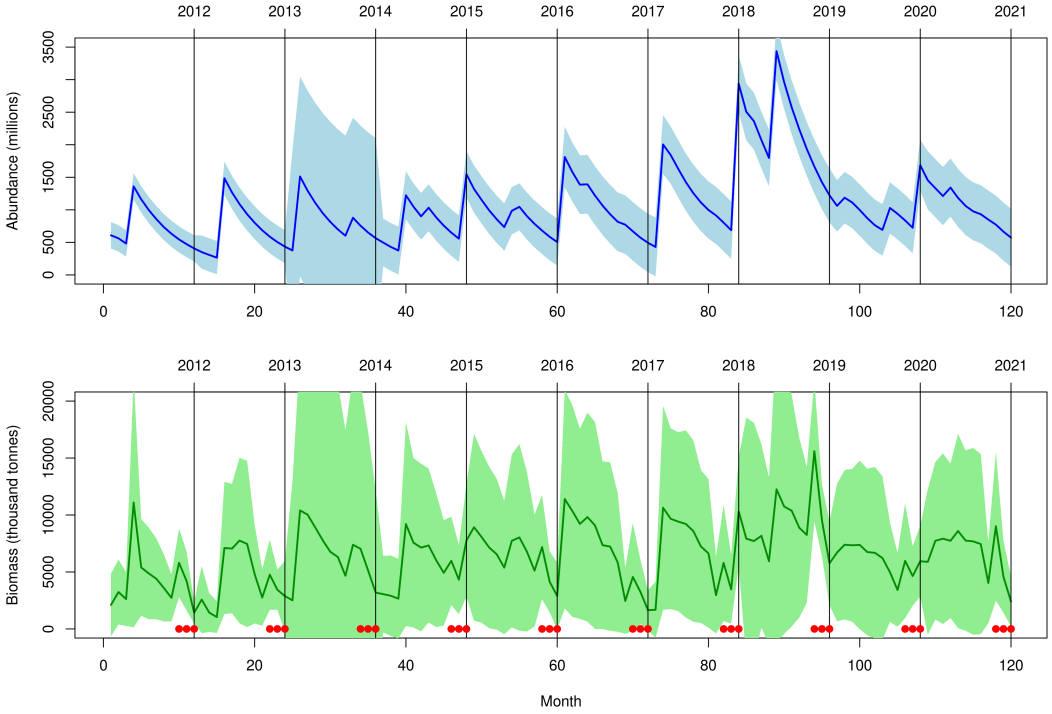

Figure 16: Predicted total abundance and biomass time series and their statistical precision in the SEP. Bands are predicted values ± 1 standard error

3.2 Population dynamics models

Only three out of eight hypotheses for Pella-Tomlinson dynamics (Eqs. 4 and 5) produced successful convergence in ADMB. These were the null hypothesis of no change in parameters due to the environmental cycle and the hypotheses of change in either the symmetry of the production function p or the intrinsic rate of population growth (Table 2). Although all three variants are tied on the AIC (differences not larger than 2), Alternative 2 has the most realistic measures of statistical precision so we provisionally select this variant as the most supported model of the biomass dynamics.

The best supported Pella-Tomlinson model shows a stock that started to undergo severe fluctuations when the environment switched from normal to El Niño and fishing removals started to rise in the 90s (Fig. 17). Currently the stock is under the regime of fluctuations while landings are close to the estimated sustainable harvest rates.

Table 2: Hypotheses for population dynamics and productivity of the jumbo squid stock in the SEP under Pella-Tomlinson biomass dynamics and environmental cycles. The best supported hypothesis is highlighted in color.

Hypothesis	max. $\lvert gradient \rvert$	**AIC**	**Nº pars.**	**Parameter**	**M.L.E.**	**CV (%)**
Null	<0.01	-315	3	K (tonnes)	5,457,500	40.5
				p	2.8257	112.7
				r (1/year)	0.6067	20.9
Alternative 1	<0.01	-313	4	K (tonnes)	5,426,900	30.6
				p_1	1.6487	0.4
				p_2	2.0960	96.3
				r (1/year)	1.0942	0.9
Alternative 2	<0.01	-313	4	K (tonnes)	5,286,500	20.5
				p	2.0268	29.9
				r_1 (1/year)	1.8120	65.8
				r_2 (1/year)	3.3936	49.2

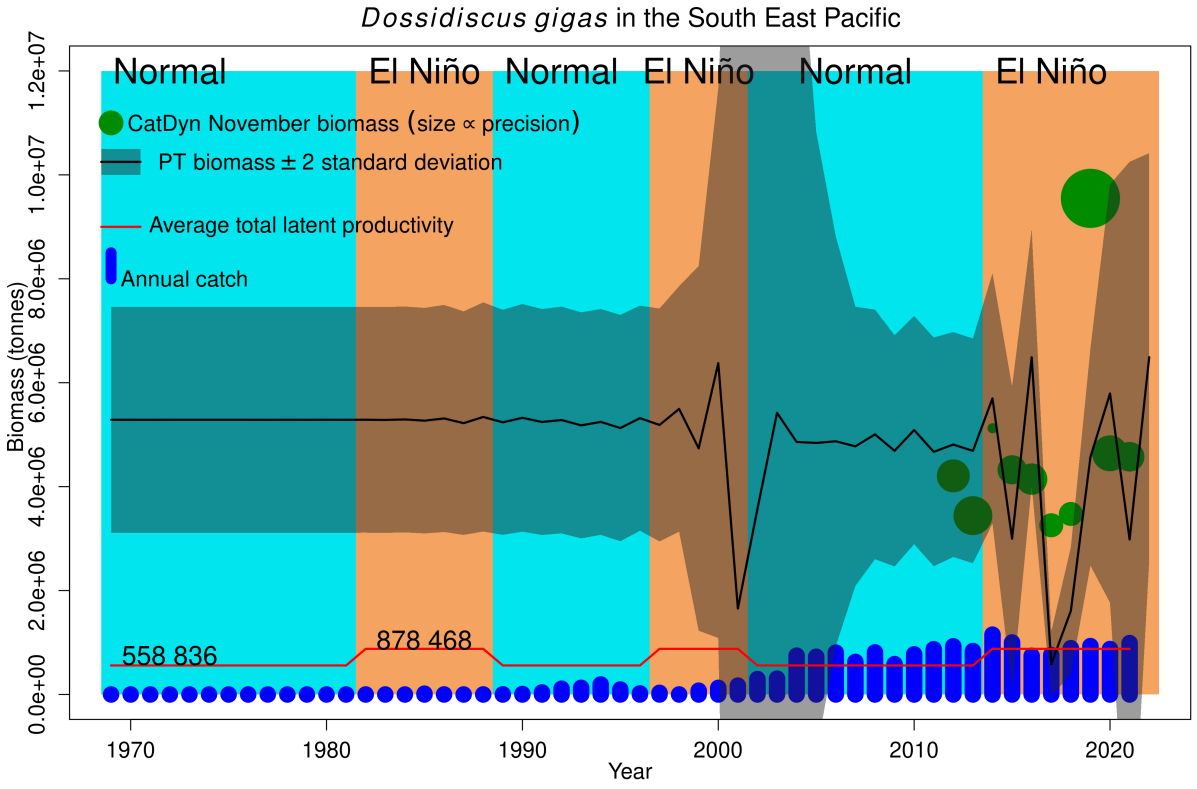

Figure 17: November stock biomass estimated by the best depletion model, biomass dynamics from the best Pella-Tomlinson model, total regional catch by Peruvian, Asian, and Chilean fleets, and sustainable harvest rates calculated from the average total latent productivity of the jumbo squid fishery in the South-Eastern Pacific.

Due to fluctuations, the MSY and B_{MSY} are not adequate reference points. This fact manifests itself in very high MSY estimates (Table 3) during both phases of the environmental cycle. The total average latent productivity, proposed as the adequate limit harvest rate and generator of biological reference points for fluctuating stocks [23], provides much more conservative estimates which are in line with recent actual landings (Table 3 and Fig. 17). Statistical precision of the total average latent productivity is still poor because it depends on biomass estimates as well as parameter estimates for K, p and r. Statistical precision of the total average latent productivity will improve as more years of fishing are added to the database to fit the depletion model.

Table 3: Derived parameters of interest (biological reference points) for management from the best supported Pella-Tomlinson model (MSY, B_{MSY}, and $\dot{P}$) for the jumbo squid in the SEP according to parameterization in Eq. 5. $\dot{P}$ is the annually averaged total latent productivity under the normal and El Niño environmental cycle.

Regime	**Parameter**	**Estimate**	**CV** (%)
Normal	MSY (tonnes)	2,438,925	21.4
	B_{MSY} (tonnes)	2,656,839	31.1
	$\dot{P}$ (tonnes)	558,835	354.5
	Mean annual landings (tonnes)	262,315	132.1
El Niño	MSY (tonnes)	4,567,735	11.8
	B_{MSY} (tonnes)	2,656,839	71.3
	$\dot{P}$ (tonnes)	878,468	389.3
	Mean annual landings (tonnes)	408,736	111.6

Overall, results of both the depletion model as well as the surplus production model indicate that the stock is being harvested in a sustainable manner, although at close to limit capacity and with wide intra- and inter-annual fluctuations in biomass, which are a matter of concern (Fig. 17).

4 Discussion

The stock assessment methodology implemented in this work shows that it is possible to understand the population dynamics of the jumbo squid in the Southern Eastern Pacific Ocean (SEP) and derive biological references points at the regional level with data consisting of monthly total catch, fishing effort and samples of the mean weight of squids in the catch from all fleets participating in the fishery. The main improvements of this work compared with our last assessment with this methodology [47] are (utilization of dis-aggregated, official (i) Peruvian catch, effort and biological data and (i) Chinese biological data. These contributions allowed development and implementation of the three-fleets depletion model at stage 1. These improvements in the data resulted in more precise and realistic natural mortality rate and abundance estimates from the depletion model. In turn, improvements

in the depletion model outputs contributed to improved biological realism and statistical precision at the level of the surplus production model.

Further improvement of the database for stock assessment using our methodology could be achieved by updating the data regarding catch, effort and monthly weight across all fleets to 2022. Current availability of data up to 2022 includes the Chilean and Asian fleets, while Peruvian data are available up to 2021. A fully updated database will contribute to a longer time series of abundances estimated by the depletion model, thus, extending the number of observations of biomass for estimation of the surplus production model. Completing the Ecuadorian database would also help providing the methodology with more data and assess the part of the stock inside Ecuadorian EEZ. Although the Ecuadorian share of the catches is small, Ecuadorian fleets operate in a large area not covered by the present assessment. These data unfortunately appears not to be available prior to 2018. Nevertheless, the methodology can be adapted to accept a time series of Ecuadorian fishing starting in January 2018 and extending to the present.

We modeled the impact of El Niño environmental cycle under fixed settings for start and end of each phase of the cycle. This can be improved in at least two ways. First, we can evaluate different oceanographic indicators for hypotheses of the timings of start and end of each phase of the environmental cycle. A few different oceanographic indicators have been used to assess regimen shifts in the East Pacific [48, 49] and the spatial scale involved on such indicators is also relevant when evaluating the length (period) of these environmental phases [26, 50]. Our modeling framework is flexible enough to implement and test hypotheses for environmental phases with different timings. Second, the modeling approach also allows setting fuzzy starts and ends of each phase by introducing continuous-time changes in parameters at the borders of the phases. We employed such approach under a similar modeling framework to estimate the impact of deployment of artificial reefs in the Algarve, Portugal [21]. This second improvement would probably require a much longer time series of biomass estimates from the depletion model because it introduces new parameters to be estimated, parameters that control the continuity of change across borders of the phases of the environmental cycle.

The Humboldt Current Ecosystem (HCE) is perturbed by different oceanographic conditions, providing environmental variability on a wide variety of temporal and spatial scales. The HCE is often perturbed by El Niño, which is a result of a complex combination of oceanic-atmospheric coupling [51], resulting in changes in the physico-chemical conditions of the water column (temperature, salinity, oxygen, and others), a rising sea level, upwelling weakness, thermocline deepness, and variations in primary production and larval food spectrum [52, 53, 54]. In the context of the jumbo squid stock, the bulk of scientific evidence is showing that El Niño affects functioning at the individual and at the population levels. At the individual level, El Niño favors the smaller phenotypes off Peru whereas on colder periods the larger phenotypes are more predominant [55], which we confirm here with a higher intrinsic rate of population growth during El Niño (Table 2. At the population level, El Niño induce a shrink in the suitable habitat for jumbo squid [56], lowering the overall population abundance, which we could not confirm in this work because models with varying carrying capacity could not achieve successful convergence in ADMB. We expect to find decreased carrying capacity during El Niño once the time series of biomass estimates from depletion

models gets sufficiently long.

These outcomes at the individual and population functioning levels of the jumbo squid stock are in line with the general theory of size-temperature rule [57], in which higher temperature will result in higher metabolic rates, smaller individuals at a given age and lower asymptotic length. Life history theory at the individual level is also mirrored with what happens at the population level [58] and thus higher temperature results in higher intrinsic growth rate and lower carrying capacity.

In jumbo squids, the effects of the El Niño not only produced smaller individuals and lower abundance levels but also increased the variability of the abundance (Fig. 17). During warm, El Niño periods, the stock experiences wider fluctuations in abundance compared with cold, normal periods of the environmental cycle. This agree with the general theory for population fluctuations proposed by Segura et al [59]. This theory uses basic and general principles in ecology to show that variability of the population abundance depends on two factors, the mean individual size of animals in the population and the level of harvesting (exploitation). Smaller average individuals in the population will produce wider population fluctuations. Fishing exploitation increase this variability. For example, exploited fish populations showed variability that was 2 orders of magnitude greater than the non-exploited counterparts [59] at a given average body size. Therefore we would expect that during warm El Niño phases of the environmental cycle, individuals of jumbo squid will be smaller, triggering wider populations fluctuations, which will also increase by fishing exploitation.

The existence of three phenotypes of the jumbo squid across the region [60] is an important component of the biological composition of the stock and taking this into account may improve the biological realism of any stock assessment model. Within the context of our approach to stock assessment this can be achieved potentially to a great extent by allowing natural mortality rate to vary among the fleets in the depletion model. Operationally, it is possible to make the natural mortality rate be fleet specific, having a different value to estimate for each of the three components if the sum of the last line of eq. 1. This would be justified on the facts that (1) the three fleets operate in different areas and (2) the size composition of their catches is different (Fig. 2. This improvement would be in line with the views of IMARPE [61], which pointed out to natural mortality as one of the factors distinguishing the phenotypes. In the next application of our methodology we plan to include this improvement in the depletion model.

Since fishery removals have apparently reached a level of maximum stock capacity and the stock has entered into a regime of wide fluctuations in abundance, we expect that landings as well will soon enter a period of wide fluctuations, just as it happened in the Argentine longfin squid (*Illex argentinus*) in 2000 and the subsequent two decades.

Sustainable harvest rates have been estimated based on the concept of the total latent productivity. These harvest rates are very close to current harvest rates but they suffer from poor statistical precision due to a relatively short time series of biomass estimates from the depletion model. Precision wikll get better as more years are added to the database.

5 Conclusions

1. A regional stock assessment methodology for the jumbo squid in the South East Pacific Ocean based on monthly effort, catch and mean weight data from three fleets (Peruvian, Asian high seas, and Chilean) and consisting of two stages has been developed and implemented with biologically realistic results and reasonable statistical precision, except for sustainable harvest rates.

2. Natural mortality was estimated in 1.8516 per year. Fishing mortality is much lower than natural mortality and has been increasing in recent years, with an annually aggregated exploitation rate ($catch \div escapement\ biomass$) close to 15% in latest years.

3. Biomass has wide intra-annual fluctuations, with maxima near March 4 times the size of minima near September, but it has remained fluctuating about a constant mean.

4. Analysis of the NOAA ENSO indicator of El Niño determined the existence of an environmental cycle with six phases during the period of our assessment, 1969 to 2020.

5. The biomass dynamics of the stock in the region is driven by environmental cycles connected to El Niño, leading to changes in the carrying capacity of the environment.

6. During warm, El Niño years the stock has lower carrying capacity and wider fluctuations than during normal, cold water periods.

7. Actual harvest rates during warm, El Niño years as well during cold, normal periods have been well below the sustainable harvest rates of each period.

8. Wide intra-annual fluctuations in biomass should be taken into account when managing the jumbo squid stock in the SEP.

9. Results from depletion models (high escapement biomass) and surplus production model (catches well below limit sustainable harvest rates) indicate that the stock is not overfished and not undergoing over-fishing.

List of Figures

List of Tables

References

[1] C. J. Robinson, J. Gómez-Gutiérrez, U. Markaida, and W. F. Gilly, "Prolonged decline of jumbo squid (dosidicus gigas) landings in the gulf of california is associated with chronically low wind stress and decreased chlorophyll a after el niño 2009–2010," *Fisheries Research*, vol. 173, pp. 128–138, 2016.

[2] W. F. Gilly, C. A. Elliger, C. A. Salinas, S. Camarilla-Coop, G. Bazzino, and M. Beman, "Spawning by jumbo squid dosidicus gigas in san pedro mártir basin, gulf of california, mexico," *Marine Ecology Progress Series*, vol. 313, pp. 125–133, 2006.

[3] C. M. and Ibáñez and L. A. Cubillos, "Seasonal variation in the length structure and reproductive condition of the jumbo squid dosidicus gigas (dorbigny, 1835) off central-south chile," *Scientia Marina*, vol. 71, no. 1, pp. 123–128, 2007.

[4] T. Berger and F. Sibeni and F. Calderini, *FishStatJ*.

[5] Z. Fang, J. Li, K. Thompson, F. Hu, X. Chen, B. Liu, and Y. Chen, "Age, growth, and population structure of the red flying squid (ommastrephes bartramii) in the north pacific ocean, determined from beak microstructure.," *Fishery Bulletin*, vol. 114, no. 1, 2016.

[6] A. T. Hernández-Muñoz, C. Rodríguez-Jaramillo, A. Mejía-Rebollo, and C. A. Salinas-Zavala, "Reproductive strategy in jumbo squid dosidicus gigas (dorbigny, 1835): A new perspective," *Fisheries research*, vol. 173, pp. 145–150, 2016.

[7] S. M. Aguilar, J. A. d. A. Montañez, J. G. D. Uribe, and M. A. C. Mata, "Natural mortality and life history stage duration for the jumbo squid (dosidicus gigas) in the gulf of california, mexico, using the gnomonic time division," *Ciencia Pesquera*, 2010.

[8] R. Rosas-Luis and L. Chompoy-Salazar, "Description of food sources used by jumbo squid dosidicus gigas (dorbigny, 1835) in ecuadorian waters during 2014," *Fisheries Research*, vol. 173, pp. 139–144, 2016.

[9] R. Rosas-Luis, P. Loor-Andrade, M. Carrera-Fernández, J. Pincay-Espinoza, C. Vinces-Ortega, and L. Chompoy-Salazar, "Cephalopod species in the diet of large pelagic fish (sharks and billfishes) in ecuadorian waters," *Fisheries Research*, vol. 173, pp. 159–168, 2016.

[10] C. Paulino, M. Segura, and G. Chacón, "Spatial variability of jumbo flying squid (dosidicus gigas) fishery related to remotely sensed sst and chlorophyll-a concentration (2004-2012)," *Fisheries Research*, vol. 173, pp. 122–127, 2016.

[11] SPRFMO, "Sc 2nd squid workshop report.," tech. rep., SPRFMO: Wellington, New Zealand 2019, 2019.

[12] SPRFMO, "8th scientific committee meeting report," tech. rep., SPRFMO: Wellington, New Zealand 2020, 2020.

[13] R. Wiff and R. H. Roa-Ureta, "Regional stock assessment of flying jumbo squid in the south-eastern pacific: A conceptual proposal," tech. rep., SPRFMO: 9th MEETING OF THE SCIENTIFIC COMMITTEE, 2021.

[14] I. Payá, "First attempt to apply the stochastic production model in continuous time (spict) to d. gigas in fao87 area," tech. rep., SPRFMO: Squid Working Group presentation, 2022.

[15] P. G. Rodhouse, C. Yamashiro, and J. Arguelles, "Jumbo squid in the eastern pacific ocean: a quarter century of challenges and change," *Fisheries Research*, vol. 173, no. 2, pp. 109–112, 2016.

[16] A. I. Arkhipkin, L. C. Hendrickson, I. Payá, G. J. Pierce, R. H. Roa-Ureta, J.-P. Robin, and A. Winter, "Stock assessment and management of cephalopods: advances and challenges for short-lived fishery resources," *ICES Journal of Marine Science*, vol. 78, no. 2, pp. 714–730, 2021.

[17] H.-J. T. Hoving, V. V. Laptikhovsky, and B. H. Robison, "Vampire squid reproductive strategy is unique among coleoid cephalopods," *Current Biology*, vol. 25, no. 8, pp. R322–R323, 2015.

[18] K. Nesis, *Dosidicus gigas In: P.R. Boyle (ed.). Cephalopod life cycles, Vol. 1. Species accounts*. London: Academic Press, 1983.

[19] A. Arkhipkin and R. H. Roa-Ureta, "Identification of growth models for squids," *Marine and Freshwater Research*, vol. 56, pp. 371–386, 2005.

[20] R. H. Roa-Ureta, C. Molinet, N. Barahona, and P. Araya, "Hierarchical statistical framework to combine generalized depletion models and biomass dynamic models in the stock assessment of the Chilean sea urchin (*Loxechinus albus*) fishery," *Fisheries Research*, vol. 171, pp. 59–67, 2015.

[21] R. H. Roa-Ureta, M. N. Santos, and F. Leitao, "Modelling long-term fisheries data to resolve the attraction versus production dilemma of artificial reefs," *Ecological Modelling*, vol. 407, p. 108727, 2019.

[22] R. H. Roa-Ureta, J. Henríquez, and C. Molinet, "Achieving sustainable exploitation through co-management in three chilean small-scale fisheries," *Fisheries Research*, vol. 230, p. 105674, 2020.

[23] R. H. Roa-Ureta, M. del Pino Fernández-Rueda, J. L. A. na, A. Rivera, R. González-Gil, and L. García-Flórez, "Estimation of the spawning stock and recruitment relationship of *Octopus vulgaris* in asturias (bay of biscay) with generalized depletion models: implications for the applicability of msy," *ICES Journal of Marine Science*, p. fsab113, 2021.

[24] H.-J. T. Hoving, W. F. Gilly, U. Markaida, K. J. Benoit-Bird, Z. W. Brown, P. Daniel, J. C. Field, L. Parassenti, B. Liu, and B. Campos, "Extreme plasticity in life-history strategy allows a migratory predator (jumbo squid) to cope with a changing climate," *Global change biology*, vol. 19, no. 7, pp. 2089–2103, 2013.

[25] W. Yu, J. Wen, X. Chen, and B. Liu, "El niño–southern oscillation impacts on jumbo squid habitat: Implication for fisheries management," *Aquatic Conservation: Marine and Freshwater Ecosystems*, vol. 31, no. 8, pp. 2072–2083, 2021.

[26] A. Flores, R. Wiff, M. Ahumada, D. Queirolo, and P. Apablaza, "Coping with el niño: phenotypic flexibility of reproductive traits in red squat lobster determines recruitment success," *ICES Journal of Marine Science*, vol. 78, no. 10, pp. 3709–3723, 2021.

[27] M. Lima, T. M. Canales, R. Wiff, and J. Montero, "The interaction between stock dynamics, fishing and climate caused the collapse of the jack mackerel stock at humboldt current ecosystem," *Frontiers in Marine Science*, vol. 7, p. 123, 2020.

[28] R. H. Roa-Ureta, "Modeling in-season pulses of recruitment and hyperstability-hyperdepletion in the *Loligo gahi* fishery of the Falkland Islands with generalized depletion models," *ICES Journal of Marine Science*, vol. 69, pp. 1403–1415, 2012.

[29] R. H. Roa-Ureta, "Stock assessment of the Spanish mackerel (*Scomberomorus commerson*) in Saudi waters of the Arabian Gulf with generalized depletion models under data–limited conditions," *Fisheries Research*, vol. 171, pp. 68–77, 2015.

[30] R. H. Roa-Ureta, "A likelihood-based model of fish growth with multiple length frequency data," *Journal of Agricultural, Biological and Environmental Statistics*, vol. 15, pp. 416–429, 2010.

[31] B. Meissa, M. Dia, B. C. Baye, M. Bouzouma, E. Beibou, and R. H. Roa-Ureta, "A comparison of three data-poor stock assessment methods for the pink spiny lobster fishery in mauritania," *Frontiers in Marine Science*, vol. 8, p. 714250, 2021.

[32] S. van Buuren and K. Groothuis-Oudshoorn, "mice: Multivariate imputation by chained equations in r," *Journal of Statistical Software*, vol. 45, no. 3, pp. 1–67, 2011.

[33] Y.-J. Lin, W.-N. Tzeng, Y.-S. Han, and R. H. Roa-Ureta, "A stock assessment model for transit stock fisheries with explicit immigration and emigration dynamics: application to upstream waves of glass eels," *Fisheries Research*, vol. 195, pp. 134–140, 2017.

[34] R. H. Roa-Ureta, *CatDyn: Fishery Stock Assessment by Generalized Depletion Models*, 2019. R package version 1.1-1.

[35] H.-H. Lee, M. Maunder, K. Piner, and R. Methot, "Estimating natural mortality within a fisheries stock assessment model: An evaluation using simulation analysis based on twelve stock assessments," *Fisheries Research*, vol. 109, pp. 89–94, 2011.

[36] S. Anderson, C. Monnahan, K. Johnson, K. Ono, and J. Valero, "ss3sim: An r package for fisheries stock assessment simulation with stock synthesis," *PLoS ONE*, vol. 9(4), p. e92725, 2014.

[37] F. Hurtado-Ferro, C. Szuwalski, J. Valero, S. Anderson, C. Cunningham, K. Johnson, R. Licandeo, C. McGilliard, C. Monnahan, M. Muradian, K. Ono, K. Vert-Pre, A. Whitten, and A. Punt, "Looking in the rear-view mirror: bias and retrospective patterns in integrated, age-structured stock assessment models," *ICES Journal of Marine Science*, vol. 72, pp. 99–110, 2015.

[38] J. Thorson, A. Hicks, and R. Methot, "Random effect estimation of time-varying factors in stock synthesis," *ICES Journal of Marine Science*, vol. 72, pp. 178–185, 2015.

[39] J. Nash and R. Varadhan, "Unifying optimization algorithms to aid software system users: optimx for r," *Journal of Statistical Software*, vol. 43, pp. 1–14, 2011.

[40] C. Wang, "A review of enso theories," *National Science Review*, vol. 5, pp. 813–825, 2018.

[41] S. Yang, Z. Li, J.-Y. YU, X. Hu, W. Dong, and S. He, "El niño southern oscillation and its impact in the changing climate," *National Science Review*, vol. 5, pp. 840–857, 2018.

[42] R. Francis, "Replacing the multinomial in stock assessment models: a first step," *Fisheries Research*, vol. 151, pp. 70–84, 2014.

[43] R. Francis, "Revisiting data weighting in fisheries stock assessment models," *Fisheries Research*, vol. 192, pp. 6–15, 2017.

[44] R. D. T.J. Quinn II, *Quantitative Fish Dynamics*. New York: Oxford University Press, 1999.

[45] D. Fournier, J. Skaug, J. Ancheta, J. Ianelli, A. Magnusson, and M. Maunder, "Ad model builder: using automatic differentiation for statistical inference of highly parameterized complex nonlinear models," *Optimization Methods and Software*, vol. 27, pp. 233–249, 2012.

[46] A. Magnusson, *ADMB-IDE: Easy and efficient user interface*. ADMB Foundation, 2009.

[47] R. H. Roa-Ureta and R. Wiff, "Regional stock assessment of the flying jumbo squid in the south-eastern pacific," tech. rep., SPRFMO: 10th MEETING OF THE SCIENTIFIC COMMITTEE, 2022.

[48] J. Alheit and M. Niquen, "Regime shifts in the humboldt current ecosystem," *Progress in Oceanography*, vol. 60, no. 2-4, pp. 201–222, 2004.

[49] F. P. Chavez, J. Ryan, S. E. Lluch-Cota, and M. Ñiquen C, "From anchovies to sardines and back: multidecadal change in the pacific ocean," *science*, vol. 299, no. 5604, pp. 217–221, 2003.

[50] S. Purca Cuicapusa, *Variabilidad temporal de baja frecuencia en el Ecosistema de la Corriente Humboldt frente a Perú*. Phd thesis, Universidad de Concepción, Concepción, January 2005. Available at `http://repositorio.udec.cl/handle/11594/5572`.

[51] M. Collins, S.-I. An, W. Cai, A. Ganachaud, E. Guilyardi, F.-F. Jin, M. Jochum, M. Lengaigne, S. Power, A. Timmermann, *et al.*, "The impact of global warming on the tropical pacific ocean and el niño," *Nature Geoscience*, vol. 3, no. 6, pp. 391–397, 2010.

[52] O. Ulloa, R. Escribano, S. Hormazabal, R. A. Quinones, R. R. González, and M. Ramos, "Evolution and biological effects of the 1997–98 el nino in the upwelling ecosystem off northern chile," *Geophysical Research Letters*, vol. 28, no. 8, pp. 1591–1594, 2001.

[53] R. Escribano, G. Daneri, L. Farías, V. A. Gallardo, H. E. González, D. Gutiérrez, C. B. Lange, C. E. Morales, O. Pizarro, O. Ulloa, *et al.*, "Biological and chemical consequences of the 1997–1998 el niño in the chilean coastal upwelling system: a synthesis," *Deep Sea Research Part II: Topical Studies in Oceanography*, vol. 51, no. 20-21, pp. 2389–2411, 2004.

[54] J. A. Rutllant, I. Masotti, J. Calderón, and S. A. Vega, "A comparison of spring coastal upwelling off central chile at the extremes of the 1996–1997 enso cycle," *Continental Shelf Research*, vol. 24, no. 7-8, pp. 773–787, 2004.

[55] IMARPE, "SituaciĂłn del calamar gigante durante el 2020 y perspectivas de captura para el 2021," tech. rep., IMARPE, PERU, 2022.

[56] W. Jian, G. Jingwen, L. Ting, Z. Songling, T. Yuanyuan, C. Xinjun, and Y. Wei, "Spatio-temporal variations in the habitat of jumbo squid dosidicus gigas in the southeast pacific ocean off peru under anomalous climate conditions," *Rhhz Test*, vol. 42, no. 10, pp. 92–99, 2020.

[57] M. J. Angilletta Jr, T. D. Steury, and M. W. Sears, "Temperature, growth rate, and body size in ectotherms: fitting pieces of a life-history puzzle," *Integrative and comparative biology*, vol. 44, no. 6, pp. 498–509, 2004.

[58] R. Wiff, M. A. Barrientos, A. Segura, and A. Milessi, "The invariance of production per unit of food consumed in fish populations," *Theory in Biosciences*, vol. 136, no. 3-4, pp. 179–185, 2017.

[59] A. Segura, R. Wiff, A. Jaureguizar, A. Milessi, and G. Perera, "A macroecological perspective on the fluctuations of exploited fish populations," *Marine Ecology Progress Series*, vol. 665, pp. 177–183, 2021.

[60] C. M. Nigmatullin, K. Nesis, and A. Arkhipkin, "A review of the biology of the jumbo squid dosidicus gigas (cephalopoda: Ommastrephidae)," *Fisheries Research*, vol. 54, pp. 9–19, 2001.

[61] IMARPE-PRODUCE, "Proposal for the creation of an assessment simulation task group for the jumbo flying squid in the south eastern pscific ocean," Tech. Rep. SC11-WP02, IMARPE-PRODUCR, 2023.